


1. Report No. DOT/DF-81/005c FHWA/RD-81/070		2. Government Accession No. PB82 15737 1		PB82157371 	
4. Title and Subtitle NONCONTACT ROAD PROFILING SYSTEM VOLUME 3 - SYSTEM SOFTWARE				5. Report Date October 1981	
				6. Performing Organization Code 1300 035009	
7. Author(s) Preston G. Smith, Steven Macintyre, Ta-Lun Yang				8. Performing Organization Report No. TIS-1300-Final Report Volume 3	
9. Performing Organization Name and Address ENSCO, INC. 5400 Port Royal Road Springfield, VA 22151				10. Work Unit No. (TR AIS) 39B2-014	
				11. Contract or Grant No. DOT-FH-11-9551	
12. Sponsoring Agency Name and Address Department of Transportation Federal Highway Administration Office of Research Washington, DC 20590				13. Type of Report and Period Covered Final Report January 1979 to February 1980	
				14. Sponsoring Agency Code S01167	
15. Supplementary Notes FHWA Contract Manager Dr. Rudolph R. Hegmon (HRS-12) For Magnetic Tape see PB 82-1573 97					
16. Abstract <p>Road profiles are of interest because they affect vehicle ride quality, the wavelengths of concern ranging from 1/2 to 300 feet (0.2 to 90 m). This report pertains to a class of profile-measuring instruments in which an accelerometer measures vertical vehicle motion and a "noncontact" sensor measures vertical pavement motion - either displacement or velocity - relative to the vehicle. Specifically, a method is developed to process the accelerometer and noncontact sensor signals so as to obtain a measured profile with the following desirable qualities: (a) 1/2 to 300 foot wavelengths are recovered, (b) there is no phase distortion, (c) filtering and output are functions of distance rather than time, and (d) the output is independent of data collection speed and direction. A hybrid processing technique involving a minimal amount of analog processing is used. The digital processing, which is now done offline, makes use of symmetric finite impulse response filters. The processing algorithms are described in detail, and a variety of results are presented. The report is in four separately-bound units:</p> <p>Volume 1 - Overview and Operating Manual - FHWA/RD-81/068 Volume 2 - Calibration and Maintenance Manual - FHWA/RD-81/069* Volume 3 - System Software - FHWA/RD-81/070 Volume 4 - System Hardware - FHWA/RD-81/071*</p> <p>*Available from NTIS only.</p>					
17. Key Words Road roughness, profile measurement, hybrid processing, road profiles, digital double integration			18. Distribution Statement This document is available to the U.S. public through the National Technical Information Service, Springfield, Virginia, 22161.		
19. Security Classif. (of this report) Unclassified		20. Security Classif. (of this page) Unclassified		21. No. of Pages 108	22. Price

REPRODUCED BY:
U.S. Department of Commerce
National Technical Information Service
Springfield, Virginia 22161

METRIC CONVERSION FACTORS

APPROXIMATE CONVERSIONS FROM METRIC MEASURES

SYMBOL WHEN YOU KNOW MULTIPLY BY TO FIND SYMBOL

LENGTH

in	inches	2.5	centimeters	cm
ft	feet	30	centimeters	cm
yd	yards	0.9	meters	m
mi	miles	1.6	kilometers	km

AREA

in ²	square inches	6.5	square centimeters	cm ²
ft ²	square feet	0.09	square meters	m ²
yd ²	square yards	0.6	square meters	m ²
mi ²	square miles	2.6	square kilometers	km ²
	acres	0.4	hectares	ha

MASS (weight)

oz	ounces	28	grams	g
lb	pounds	0.45	kilograms	kg
	short tons (2000 lb)	0.9	tonnes	t

VOLUME

tsp	teaspoons	5	milliliters	ml
tbsp	tablespoons	15	milliliters	ml
fl oz	fluid ounces	30	milliliters	ml
c	cups	0.24	liters	l
pt	pints	0.47	liters	l
qt	quarts	0.95	liters	l
gal	gallons	3.8	liters	l
ft ³	cubic feet	0.03	cubic meters	m ³
yd ³	cubic yards	0.76	cubic meters	m ³

TEMPERATURE (exact)

°F	Fahrenheit temperature	5/9 (after subtracting 32)	Celsius temperature	°C
----	------------------------	----------------------------	---------------------	----

APPROXIMATE CONVERSIONS FROM METRIC MEASURES

SYMBOL WHEN YOU KNOW MULTIPLY BY TO FIND SYMBOL

LENGTH

m	millimeters	0.04	inches	in
cm	centimeters	0.4	inches	in
m	meters	3.3	feet	ft
m	meters	1.1	yards	yd
km	kilometers	0.6	miles	mi

AREA

cm ²	square centimeters	0.16	square inches	in ²
m ²	square meters	1.2	square yards	yd ²
km ²	square kilometers	0.4	square miles	mi ²
ha	hectares (10,000m ²)	2.5	acres	

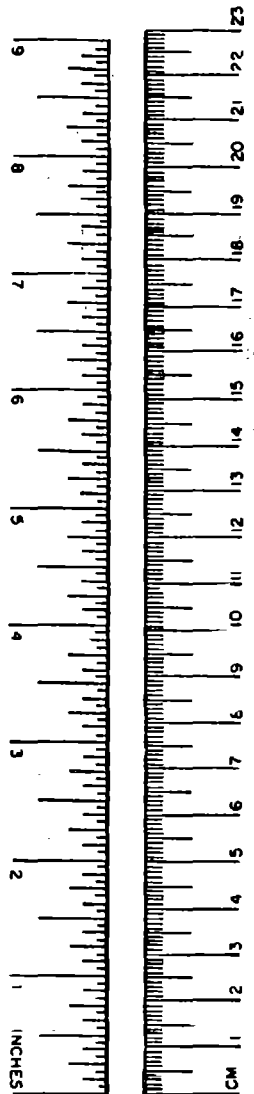
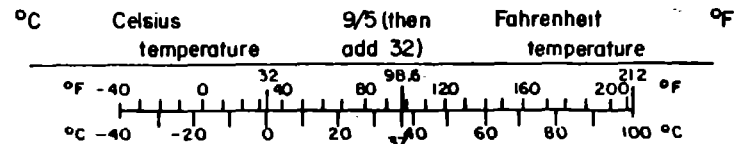
MASS (weight)

g	grams	0.035	ounces	oz
kg	kilograms	2.2	pounds	lb
t	tonnes (1000kg)	1.1	short tons	

VOLUME

ml	milliliters	8.03	fluid ounces	fl oz
l	liters	2.1	pints	pt
l	liters	1.06	quarts	qt
l	liters	0.26	gallons	gal
m ³	cubic meters	36	cubic feet	ft ³
m ³	cubic meters	1.3	cubic yards	yd ³

TEMPERATURE (exact)



GENERAL DISCLAIMER

This document may be affected by one or more of the following statements

- **This document has been reproduced from the best copy furnished by the sponsoring agency. It is being released in the interest of making available as much information as possible.**
- **This document may contain data which exceeds the sheet parameters. It was furnished in this condition by the sponsoring agency and is the best copy available.**
- **This document may contain tone-on-tone or color graphs, charts and/or pictures which have been reproduced in black and white.**
- **This document is paginated as submitted by the original source.**
- **Portions of this document are not fully legible due to the historical nature of some of the material. However, it is the best reproduction available from the original submission.**

1
2
3
4
5
6
7
8
9
10
11
12
13
14
15
16
17
18
19
20
21
22
23
24
25
26
27
28
29
30
31
32
33
34
35
36
37
38
39
40
41
42
43
44
45
46
47
48
49
50
51
52
53
54
55
56
57
58
59
60
61
62
63
64
65
66
67
68
69
70
71
72
73
74
75
76
77
78
79
80
81
82
83
84
85
86
87
88
89
90
91
92
93
94
95
96
97
98
99
100

TABLE OF CONTENTS

<u>Section</u>	<u>Title</u>	<u>Page</u>
1.0	INTRODUCTION	1
	1.1 Rapid Travel Profilometers	1
	1.2 Difficulties in Signal Processing	4
2.0	DATA PROCESSING APPROACH	14
	2.1 General Approach	14
	2.2 Specific Approach	15
3.0	PHASE JUMP PROCESSING	19
	3.1 Introduction	19
	3.2 Phase Jump Characteristics	19
	3.3 Phase Jump Detection	21
	3.4 Phase Jump Correlation	21
4.0	SECOND FINITE DIFFERENCE PROCESSING	23
	4.1 Introduction	23
	4.2 Generation of the SFD	23
	4.3 Conversion to Distance-Based Sampling	26
	4.4 Combining the Accelerometer and Noncontact Sensor Signals	27
	4.5 Computer Implementation	29
5.0	SPACE CURVE PROCESSING	35
	5.1 Introduction	35
	5.2 Fundamentals of Filtering	35
	5.3 Double Integration	45
	5.4 Final Debiasing	46
	5.5 An Example	55
	5.6 Real Time Implementation of the Algorithm	57
6.0	THE COMPUTER PROGRAM	59
	6.1 Program Structure and Subroutines	59
	6.2 Input Data	61
	6.3 Output Data	66
	6.4 Program Constants	66
	6.5 Source Code	66
	6.6 Common Blocks	66

TABLE OF CONTENTS (cont.)

<u>Section</u>	<u>Title</u>	<u>Page</u>
7.0	RESULTS	67
	7.1 Equipment Setup	67
	7.2 Data Available	68
	7.3 Phase Jump Results	70
	7.4 Profile Amplitude Results	73
	7.5 Signal Cancellation Results	76
	7.6 Space Curve Filtering Results	77
8.0	CONCLUSIONS	85
9.0	RECOMMENDATIONS	87
APPENDIX A	CALCULATION OF THE ACCELERATION BIAS	89
APPENDIX B	COMPUTER PROGRAM SOURCE LISTINGS	90
APPENDIX C	COMPUTER PROGRAM COMMON BLOCKS	99

LIST OF ILLUSTRATIONS

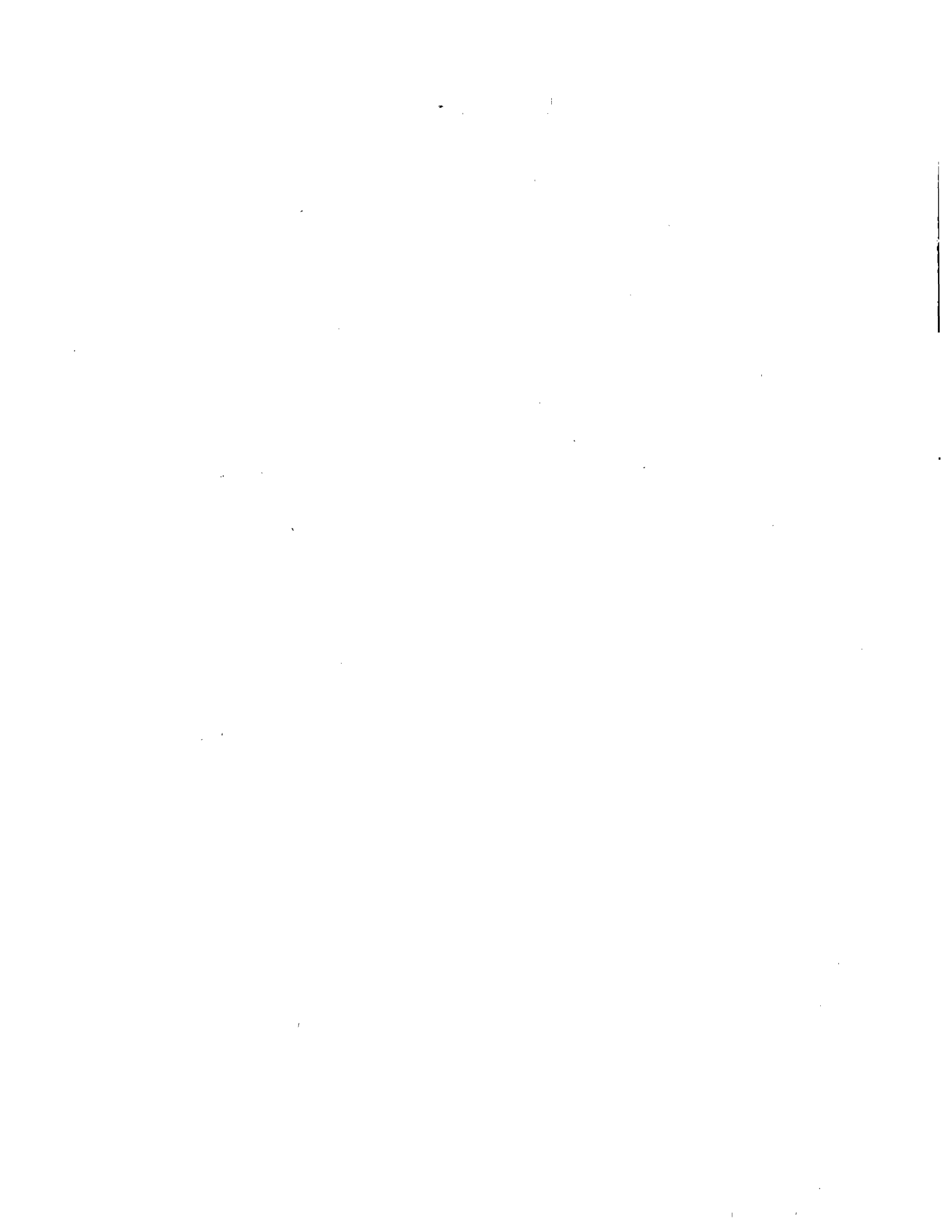
<u>Figure No.</u>	<u>Title</u>	<u>Page</u>
1	Rapid Travel Profilometer Concept	2
2	Comparison of Amplitude, Phase and Impulse Responses for Ideal vs. Approximate Analog Double Integrators	7
3	Grade Angle and Height Profile for U.S. Route 50 Between Gallows Road and Fairfax Circle, VA, as a Function Distance	11
4	Conceptual Block Diagram of Digital Processing for Acoustic Probe Input (Displacement Input Mode)	16
5	Characteristics of the Two Types of Phase Jumps	20
6	Typical Data	36
7	Impulse Response of Averaging	38
8	Impulse Response of Debiasing	39
9	Frequency Response of Filters U and W	41
10	Frequency Response of Simple and Higher Order Filters (N = 255)	42
11	Response Comparison for Various Orders of Filters	43
12	Impulse Responses for Filtering and Integration Operations	47
13	Impulse Responses for the Final Debiasing	50
14	Frequency Response With and Without Debiasing (N = 255)	53
15	Flowchart of Main Program	62

LIST OF ILLUSTRATIONS (cont.)

<u>Figure No.</u>	<u>Title</u>	<u>Page</u>
16	Phase Jump Processing for Runs 4-6	71
17	Time-based Enlargements of Three Regions in Figure 16c.	72
18	Range Extender Performance	74
19	Signal Cancellation Results	78
20	SFD Traces for Alternative Filters Having the Same Cutoff Wavelength (All are Plotted to the Same Scale)	83

LIST OF TABLES

<u>Table No.</u>	<u>Title</u>	<u>Page</u>
1	Frequency Response Characteristics of Space Curve Filtering	54
2	Space Curve Cutoff Wavelength (In Feet)	54
3	Calculation of Space Curve Impulse Response for $N = 7$	56
4	Characteristics of the Six Runs	69
5	Profile Amplitude Results	75
6	Space Curve Filter Cutoff Results	80



1.0 INTRODUCTION

This part of the report describes in detail the data processing techniques developed for the noncontact highway profilometer. The associated offline computer program is also described, and results obtained using this program are presented. Finally, this volume contains conclusions and recommendations for the project as a whole.

Part 1 of this report - Overview and Operating Manual - is intended to serve as an introduction to the detailed software description provided in this volume. Although the software itself is described in detail here, actual operation and calibration of the computer program is described in Parts 1 and 2, respectively, of this report.

1.1 RAPID TRAVEL PROFILOMETERS

Road roughness broadly refers to an uneven, unrepaired, or bumpy roadway. The roughness of highway pavements is a direct indicator of surface deterioration and directly affects vehicle component fatigue, vehicle stability, driver control, and passenger comfort. Roughness is undesirable and is distinguished from the fine-grained variations, known as texture, that are designed into pavements to provide skid resistance.

Roughness can be measured from a moving vehicle by using a rapid travel profilometer, which is conceptually illustrated in Figure 1. A displacement transducer is used to measure the relative motion between the pavement and a mass. For highway profilometers, the mass is usually the vehicle body. The mass's acceleration is measured in order to determine its motion and thus provide a profile measurement relative to an inertial reference frame.

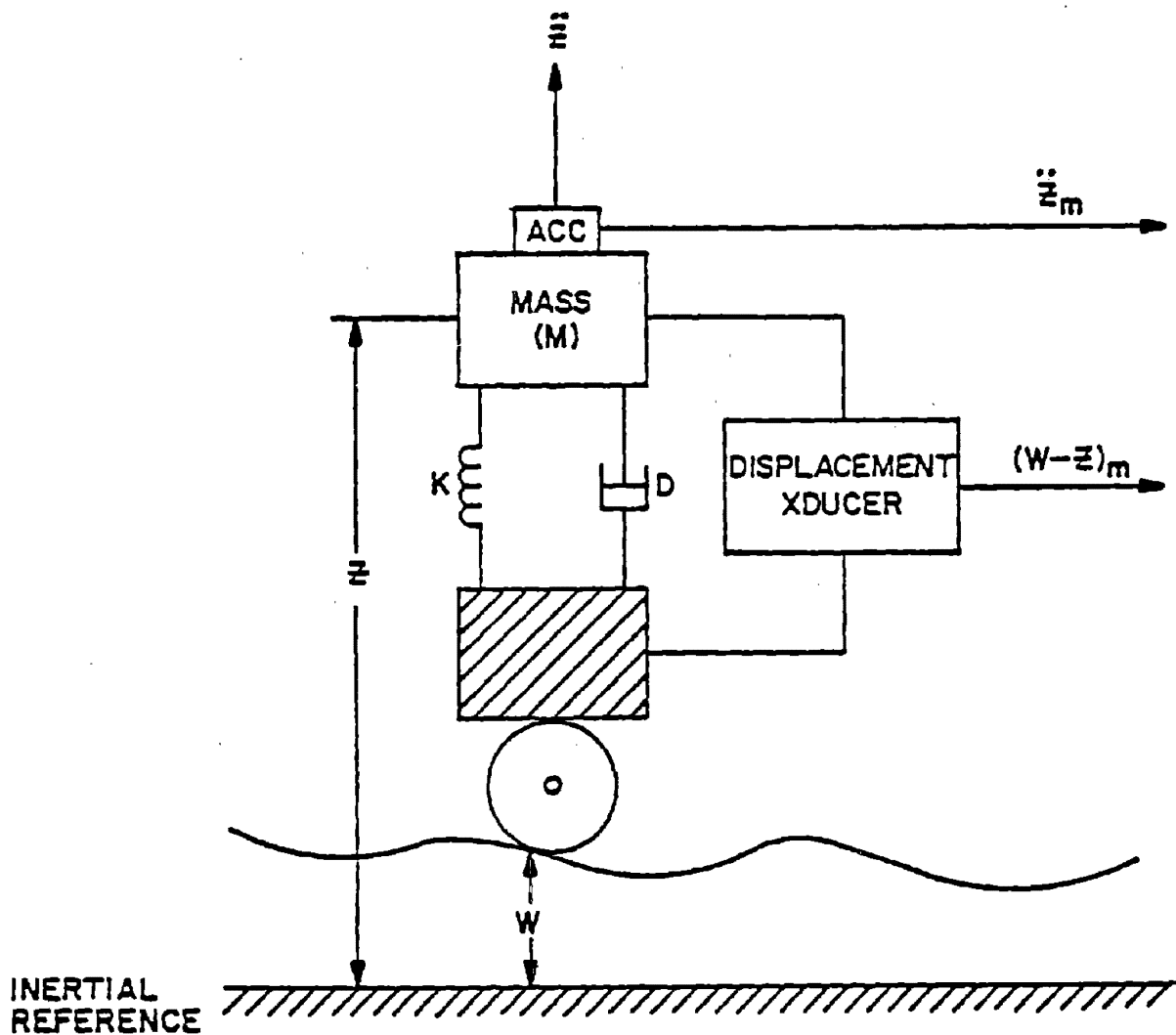


Figure 1. Rapid Travel Profilometer Concept

Some rapid travel profilometers actually use a wheel and a linear motion transducer for the relative motion measurement, as indicated in Figure 1. These include the General Motors road profilometer¹, which uses a separate measurement wheel connected to the vehicle through a linear potentiometer, and the ENSCO

¹E.B. Spangler and W. J. Kelly, "GMR Road Profilometer - A Method for Measuring Road Profile," Highway Research Record 121, Highway Research Board, 1966.

rail profilometer², which uses one of the vehicle's wheels. The difficulty with using wheels is that their mass and compliance limit the speeds and wavelengths for which profiles can be measured accurately.

As an alternative to wheels, the Federal Highway Administration (FHWA) has developed a noncontact sensor that measures the distance between the surface and the mass acoustically. The noncontact sensor, called an acoustic probe, is described in FHWA reports^{3,4} and discussed briefly in Part 1 of this report. The acoustic probe produces a phase angle output that is designed to be proportional to the displacement input. (The extent to which the output is actually proportional to the input is discussed in Section 7.4 of this report.)

Only two characteristics of the acoustic probe are pertinent to the data processing techniques discussed here. One characteristic is that the phase meter, which measures the output phase angle, has limited high frequency capability. This limitation will cause phase and amplitude distortion of short wavelength pavement profiles measured at high speed (see the Joyce report cited earlier and the ENSCO letter report⁵). The other pertinent characteristic is that the output phase angle has a range limited to 0-360 degrees. When the phase exceeds 360 degrees, the output jumps to zero and starts over, and similarly when the phase

²E. L. Brandenburg and T. J. Rudd, "Development of an Inertial Profilometer," Report FRA-ORD&D-75-15, Federal Railroad Administration, November 1974.

³R. P. Joyce, "Development of a Noncontact Profiling System," Report FHWA-RD-75-36, January 3, 1975.

⁴J. C. Wambold, "The Evaluation of a Noncontact Profiling System Using the Acoustic Probe," Report FHWA-RD-78-45, March 1978, (also published in Public Roads, December 1979, pp. 106-113).

⁵T. J. Rudd, letter to R. R. Hegmon, FHWA, regarding contract DOT-HS-11-9551, August 30, 1979.

falls below 0 degrees. Consequently, downstream processing - either analog or digital - must detect and compensate for the phase jumps.

The data processing techniques discussed below can be used with any relative motion sensor besides the acoustic probe, whether it is of the contact or noncontact type. The sensor may detect displacement, as the acoustic probe does, or velocity, as a Doppler device would.

1.2 DIFFICULTIES IN SIGNAL PROCESSING

Two types of difficulties arise in processing the accelerometer signals from a rapid travel profilometer (\ddot{z} in Figure 1):

- As the vehicle orientation changes in pitch (grade) or roll (cross slope), the effect of gravity on the accelerometer sensitive axis changes, thereby inducing an undesired acceleration signal indistinguishable from the desired vertical vehicle acceleration.
- The accelerometer signal must be double integrated in order to obtain the required vertical vehicle motion. Although double integration is simple in concept, in practice the double integration of a signal containing noise and bias - as all real signals do - will lead to an unbounded result. Filtering is necessary to suppress the noise and bias, but filtering introduces other types of errors into the signal.

These two difficulties are discussed in detail below, the double integration difficulty first because it influences the orientation difficulty.

1.2.1 DOUBLE INTEGRATION DIFFICULTY

Ideal double integration has a radian frequency response given by

$$H(i\omega) = - \frac{1}{\omega^2} \quad (1)$$

and an impulse response given by

$$h(t) = \begin{cases} t, & t > 0 \\ 0, & t \leq 0. \end{cases} \quad (2)$$

The frequency amplitude and phase responses and the impulse response of ideal double integration are illustrated by the solid lines in Figure 2. Note that

$$\lim_{\omega \rightarrow 0} H(i\omega) \rightarrow -\infty \quad (3)$$

and that the convolution

$$z(t) = \int_{-\infty}^t h(t-\tau) \ddot{z}(\tau) d\tau \quad (4)$$

contains the unbounded function $h(t-\tau)$. Therefore, this integral is mathematically improper and it does not generally converge, particularly when $\ddot{z}(\tau)$ is contaminated by noise and error signals.

This problem can be circumvented by processing the accelerometer data with an approximate double integrator whose radian frequency response is given by⁶

$$H'(i\omega) = \frac{i\omega}{(i\omega + \alpha)(-\omega^2 + i\omega\alpha + \alpha^2)} \quad (5)$$

The corresponding impulse response is

$$h'(t) = \begin{cases} \frac{1}{\alpha} \exp(-\frac{1}{2}\alpha t) [\cos(\beta t) + \frac{\alpha}{2\beta} \sin(\beta t) - \exp(-\frac{1}{2}\alpha t)], & t > 0 \\ 0, & t \leq 0 \end{cases} \quad (6)$$

⁶A simpler double integrator, namely $H'(i\omega) = 1/(-\omega^2 + i\omega\alpha + \alpha^2)$, would also provide bounded response. The advantage of the form given is that there is zero net area under $h'(t)$, which is beneficial for removing bias from the accelerometer signal.

where

$$\beta = \sqrt{\frac{5}{4}} \alpha . \quad (7)$$

Parameter α defines a radian cutoff frequency such that wavelengths longer than $2\pi V/\alpha$ are ignored, where V is the data collection speed. The responses of this approximate double integrator are illustrated by the dashed lines in Figure 2. Note that the ideal and approximate double integrators converge at high frequency or short wavelength.

The approximate double integrator will work well whenever the surface roughness wavelengths of interest are short relative to the cutoff wavelength, $2\pi V/\alpha$. Profile wavelengths near cutoff suffer severe phase distortion, so cutoff should be set 10 to 20 times longer than the longest wavelength of interest. There are two problems using such a long cutoff wavelength:

- insufficient noise and bias are removed from the signal for the double integration to work properly, and
- the liberal cutoff allows undesirable large-amplitude profile variations associated with the terrain to overwhelm the roughness information of interest.

It is clear that some sort of high-pass filtering (filtering that passes high frequencies or short wavelengths) is needed for satisfactory double integration, but the filtering provided by the analog filters used above is not adequate because analog filters are causal and thus introduce phase distortion.

1.2.2 ACCELEROMETER ORIENTATION DIFFICULTIES

If the vehicle is level so that the accelerometer's sensitive axis is vertical, then the accelerometer output is

$$a = \ddot{z} + g \quad (8)$$

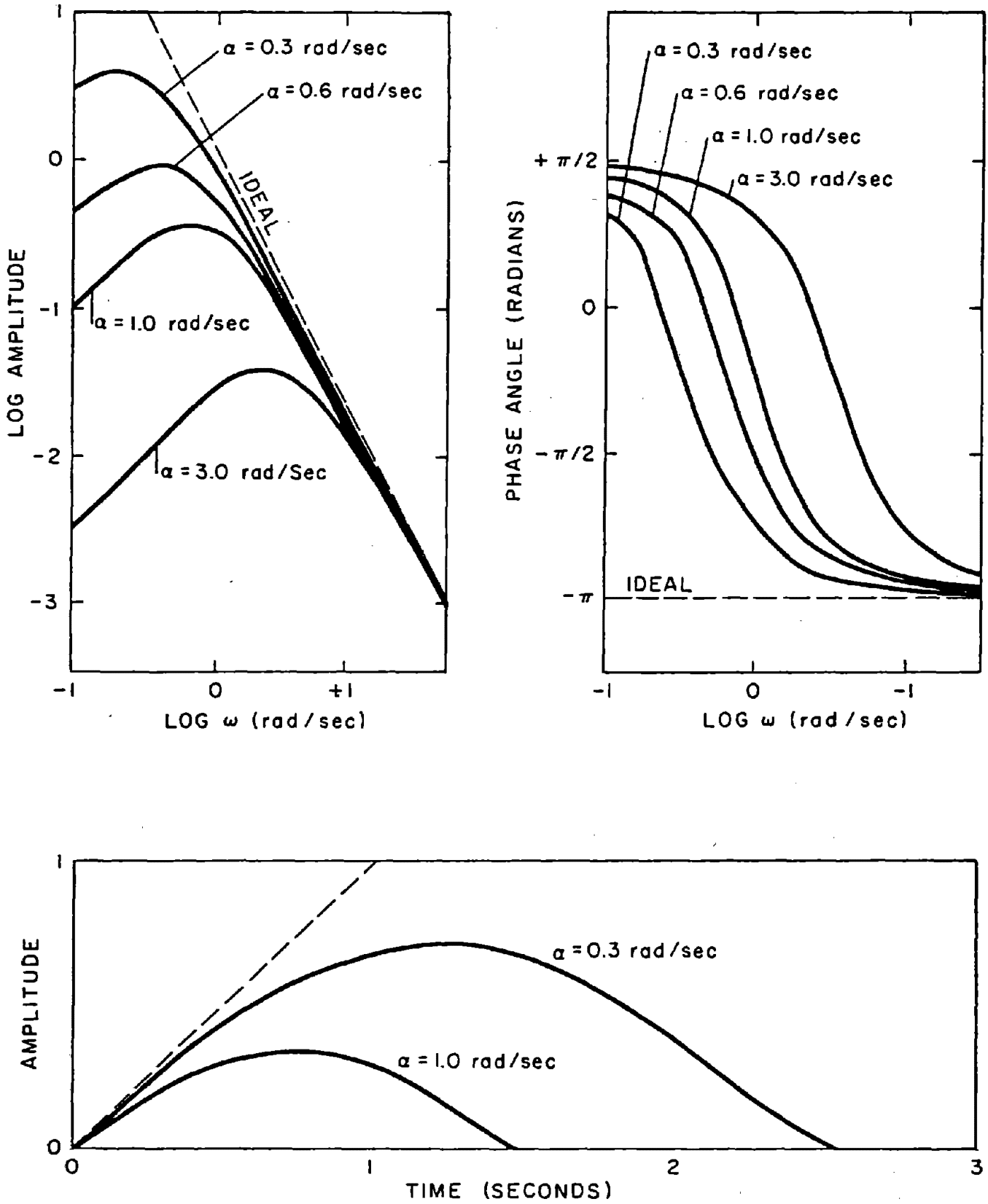


Figure 2. Comparison of Amplitude, Phase and Impulse Responses for Ideal vs. Approximate Analog Double Integrators.

where g is the acceleration due to gravity.

Accelerometers intended for vertical orientation are often biased against the 1-g input so that the output becomes

$$a = \ddot{z} . \quad (9)$$

This is exactly the theoretical output desired from an accelerometer.

If the vehicle is not level, the accelerometer's sensitive axis is not vertical, and the output of an accelerometer biased against 1-g becomes

$$a = \ddot{z} + g(\cos\theta \cos\psi - 1) \quad (10)$$

where θ is the roll (cross slope) angle and ψ is the pitch (grade) angle. These two angles are small so that

$$a \cong \ddot{z} - \frac{1}{2}g(\theta^2 + \psi^2). \quad (11)$$

Several types of nonlevel terrain can occur. One is the super-elevation designed into highway curves. Another is the vehicle roll induced by the fact that the left and right tire tracks have different pavement profiles. Highway grades are a third type.

A simple analysis of the effects of grade on measured acceleration, a , is given below in order to demonstrate the principles involved. More comprehensive analyses are needed in order to predict the magnitude of error under actual highway conditions.

Suppose that a longitudinal road profile is the combination of two sinusoids:

$$z = B_1 \sin(2\pi x/\lambda_1) + B_2 \sin(2\pi x/\lambda_2) \quad (12)$$

where

B_1, B_2 are the amplitudes of the two sinusoids,

λ_1, λ_2 are the corresponding wavelengths, and

x is distance along the road being measured.

The first sinusoid represents long wavelength grade variations, and the second represents shorter wavelengths due to pavement roughness. The corresponding pitch angle is

$$\psi = \frac{dz}{dx} = \frac{2\pi B_1}{\lambda_1} \cos(2\pi x/\lambda_1) + \frac{2\pi B_2}{\lambda_2} \cos(2\pi x/\lambda_2). \quad (13)$$

The power spectral densities of typical highway surfaces are such that B_i varies directly with λ_i , $i = 1, 2$, so that the following simplification can be used:

$$C = \frac{B_1}{\lambda_1} = \frac{B_2}{\lambda_2}. \quad (14)$$

Then

$$\psi = 2\pi C [\cos(2\pi x/\lambda_1) + \cos(2\pi x/\lambda_2)], \quad (15)$$

and

$$\begin{aligned} 1/2g\psi^2 = \pi^2 g C^2 [\cos(4\pi x/\lambda_1) + \cos(4\pi x/\lambda_2) + 2 \cos(2\pi x/\lambda_s) \\ + 2 \cos(2\pi x/\lambda_d)] \end{aligned} \quad (16)$$

where some unimportant constant terms have been dropped, and where

$$\frac{1}{\lambda_s} = \frac{1}{\lambda_1} + \frac{1}{\lambda_2}; \quad \frac{1}{\lambda_d} = \frac{1}{\lambda_1} - \frac{1}{\lambda_2}. \quad (17)$$

Equations (12) and (16) may be substituted into Equation (11) to obtain the measured acceleration, and this quantity may be double integrated to obtain the measured profile:

$$\begin{aligned}
f \text{adt} \approx & B_1 \sin(2\pi x/\lambda_1) + B_2 \sin(2\pi x/\lambda_2) \\
& + \left\{ \frac{gC^2}{4V^2} \left[\frac{\lambda_1^2}{4} \cos(4\pi x/\lambda_1) + \frac{\lambda_2^2}{4} \cos(4\pi x/\lambda_2) \right. \right. \\
& + 4\lambda_2^2 \cos(2\pi x/\lambda_1) \cos(2\pi x/\lambda_2) \\
& \left. \left. + \frac{8\lambda_2^3}{\lambda_1} \sin(2\pi x/\lambda_1) \sin(2\pi x/\lambda_2) \right] \right\} \quad (18)
\end{aligned}$$

where V is the data collection speed and the approximation arises from use of the inequality $\lambda_1 \gg \lambda_2$. The term outside of the braces, {}, is the true profile. The term inside the braces is the error term due to gravitational effects. The four error terms inside the brackets, [], are discussed in order below.

The first error term has half the wavelength of the true profile long wavelength component. The error introduced by this term, expressed as a ratio between its amplitude and the amplitude of the profile component at the same wavelength, is

$$P_1 = \frac{E_1}{B_1} = \frac{gB_1}{16V^2} \times 2 \quad (19)$$

where the factor of 2 is introduced because the contamination will affect a true profile signal component whose wavelength is one-half as long and whose amplitude is thus one-half as great.

Based on survey data for U.S. Route 50 between Gallows Road and Fairfax Circle, Fairfax County, Virginia, shown in Figure 3, a value of $B_1 = 25$ feet (7.6m) is not unreasonable for the amplitude variation of long wavelength profiles. For a data collection speed of $V = 25$ mph (40km/h), $P_1 = 0.074$, which represents a 7.4 percent error in the measured long wavelength profile. This error would not appear in the output of the digital processing, however, because the filtering associated with the double integration would suppress profile components with such long wavelengths [approximately 2500 feet (760m)]. Hence, error P_1 is not of concern.

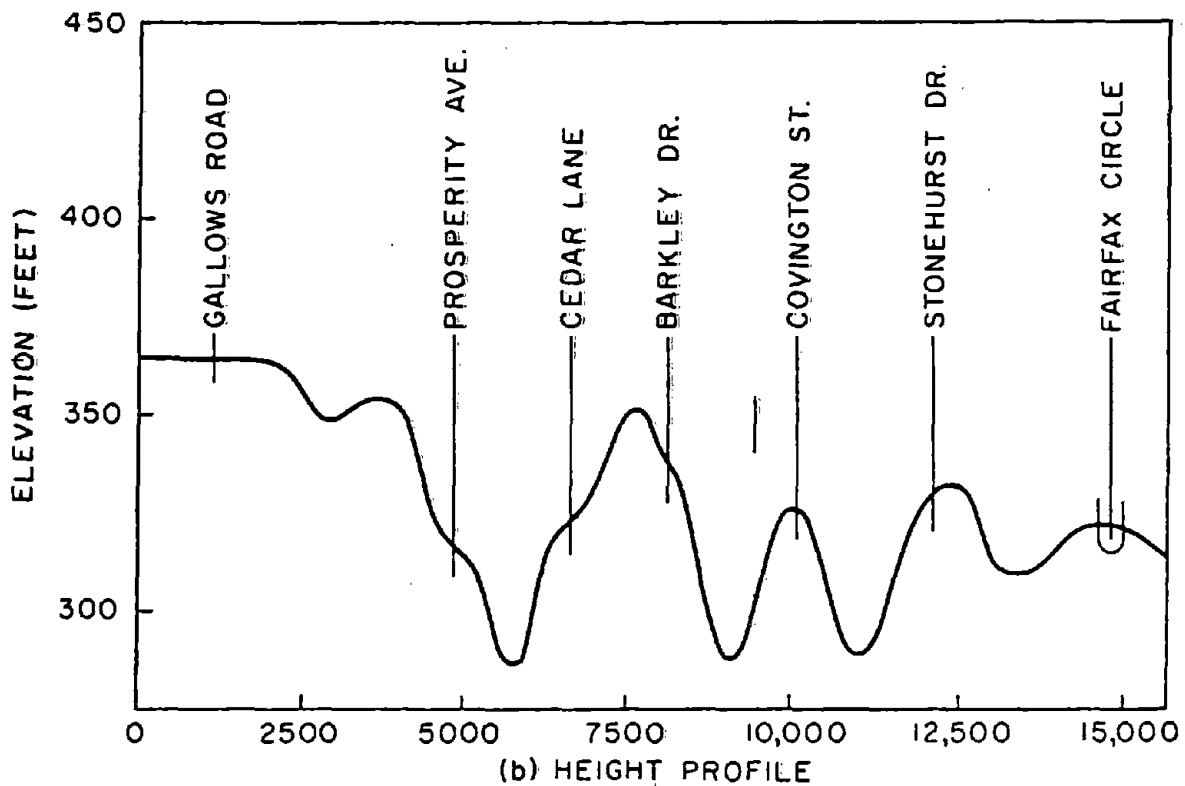
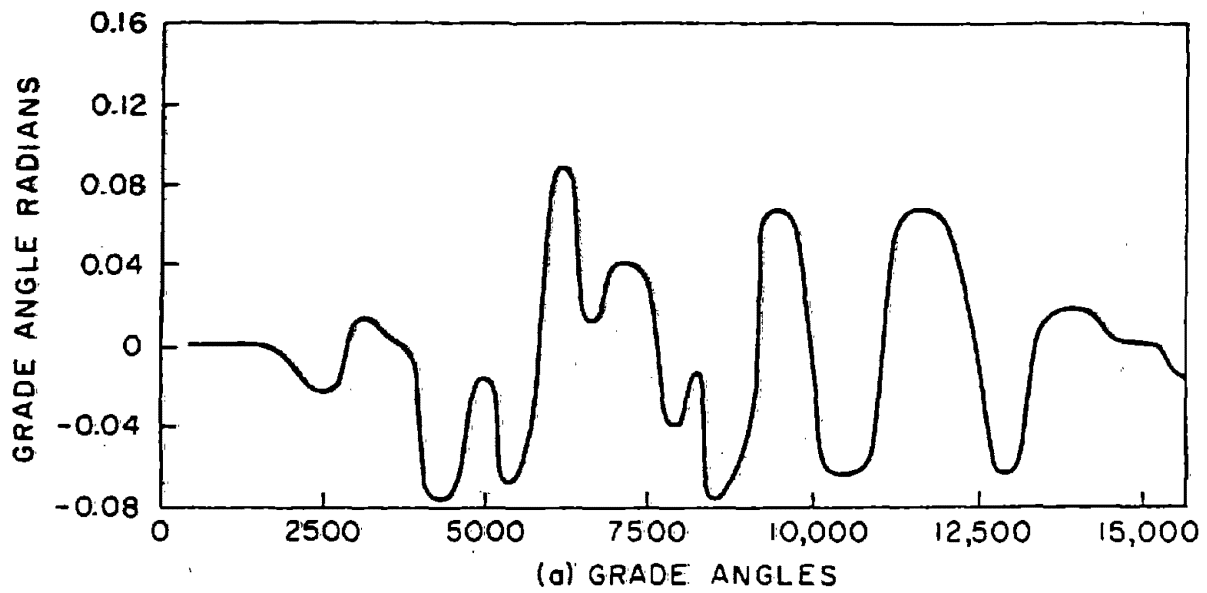


Figure 3. Grade Angle and Height Profile for U.S. Route 50 Between Gallows Road and Fairfax Circle, VA, as a Function of Distance. (Based on Coast and Geodetic Survey 1/24,000 Series Maps).

The second error term in Equation (18) is of the same form as the first, and thus the amplitude ratio of this term to the corresponding short wavelength true profile component is

$$P_2 = \frac{gB_2}{16V^2} \times 2. \quad (20)$$

Suppose that $\lambda_2 = 250$ feet (76m), which is close to the longest profile wavelength of interest in roughness measurements. Then $\lambda_1/\lambda_2 = 10$, and $B_1/B_2 = 10$ according to Equation (14). It follows that $P_2 = 0.0074$ or 0.74 percent error in the short wavelength component at 25 mph (40 km/h). This small error will appear in the output.

The third and fourth error terms in Equation (19) are more interesting. They represent amplitude modulation of the short wavelength component by the long wavelength component. When the modulation is largest ($\cos 2\pi x/\lambda_1 = 1$ and $\sin 2\pi x/\lambda_1 = 1$, respectively), the error amplitude ratios relative to the short wavelength true profile component are

$$P_3 = \frac{gB_2}{V^2} \quad (21)$$

and

$$P_4 = \frac{2gB_2\lambda_2}{V^2\lambda_1} \quad (22)$$

for the third and fourth error terms, respectively. At 25 mph (40km/h) the corresponding numerical values are $P_3 = 0.06$ (6 percent) and $P_4 = 0.012$ (1.2 percent). The third error term, because it is 90 degrees out of phase with the short wavelength true profile, increases the amplitude of the true profile by only 0.2 percent but changes its phase by 3.4 degrees. The fourth error term is in phase with the true profile, so it produces a 1.2 percent amplitude error but no phase error.

The interesting aspect of the third and fourth error terms is that although they arise from long wavelength grade variations, they appear as modulations of short wavelength roughness variations and thus cannot be removed by high pass filtering. That is, with respect to the acceleration orientation problem, the total measured pavement profile cannot be considered as the superposition of short wavelength roughness information, which could be retained, and long wavelength grade information, which could be filtered out. The reason that superposition is not valid is that the accelerometer orientation enters nonlinearly [see Equation (11)].

In general, accelerometer orientation error is proportional to $1/V^2$. This follows from the fact that the true profile measured by an accelerometer is proportional to V^2 , but accelerometer inclination is independent of V . Therefore, profilometer measurements should be made at the highest practical speed when the pavement has significant grade or cross slope variations.

Because accelerometer orientation error appears to be negligible as long as low operating speeds are avoided, no correction for this source of error is made in the data processing.

2.0 DATA PROCESSING APPROACH

2.1 GENERAL APPROACH

The data processing system described below has the following desirable qualities:

- high-pass filtering to control error in the double integration,
- high-pass filtering that introduces no phase distortion and produces results that are independent of the direction in which the data are collected (noncausal filtering),
- profile output that is distance-based rather than time-based,
- distance-based high-pass filtering so that the output is independent of data collection speed,
- selectable distance sampling interval and filters so that profile wavelengths of 1/2 to 300 feet (0.2 to 90m) can be recovered, and
- capability to accept noncontact sensor output in the form of displacement or velocity.

These qualities are obtained through hybrid processing: a minimal amount of analog filtering is done - just enough to prepare the signals properly for analog recording and digitizing - and then the bulk of the processing is done offline digitally. The advantages of digital processing are that

- symmetric, finite impulse response (FIR) filters (which are noncausal) can be used,
- it is straightforward to convert from time to distance base, and
- the filtering can be done after conversion to distance base so that the results are independent of speed.

The specific steps involved in the processing are described below.

2.2 SPECIFIC APPROACH

2.2.1 ANALOG PROCESSING

Accelerometer data, which characteristically has substantial high frequency content, poses a problem for digital processing. The high frequency portion is unnecessary for profile measurements because the displacements associated with high frequency accelerations are negligible. But the high frequency content taxes the analog data recording and digitizing processes. Therefore, some preliminary analog filtering of the accelerometer data is mandatory. It is accomplished with a double pole filter of the form

$$\omega_a^2 / (s^2 + \omega_a s + \omega_a^2)$$

No filtering of the noncontact sensor signal is needed if the sensor produces displacement data. If it produces velocity data, then a single pole filter, $\omega_v / (s + \omega_v)$, is used.

2.2.2 DIGITAL PROCESSING

The digital processing is outlined in Figure 4, which is called a conceptual block diagram because the actual processing does not divide into the convenient blocks indicated in the diagram. If a noncontact displacement sensor other than the current acoustic probe is used, then the phase jump processing indicated in the figure is not needed. If the noncontact sensor detects velocity instead of displacement, then the processing differs somewhat from that shown in the figure.

The block distance processing is described below. The phase jump, second finite difference and space curve processing are discussed in Sections 3-5, respectively.

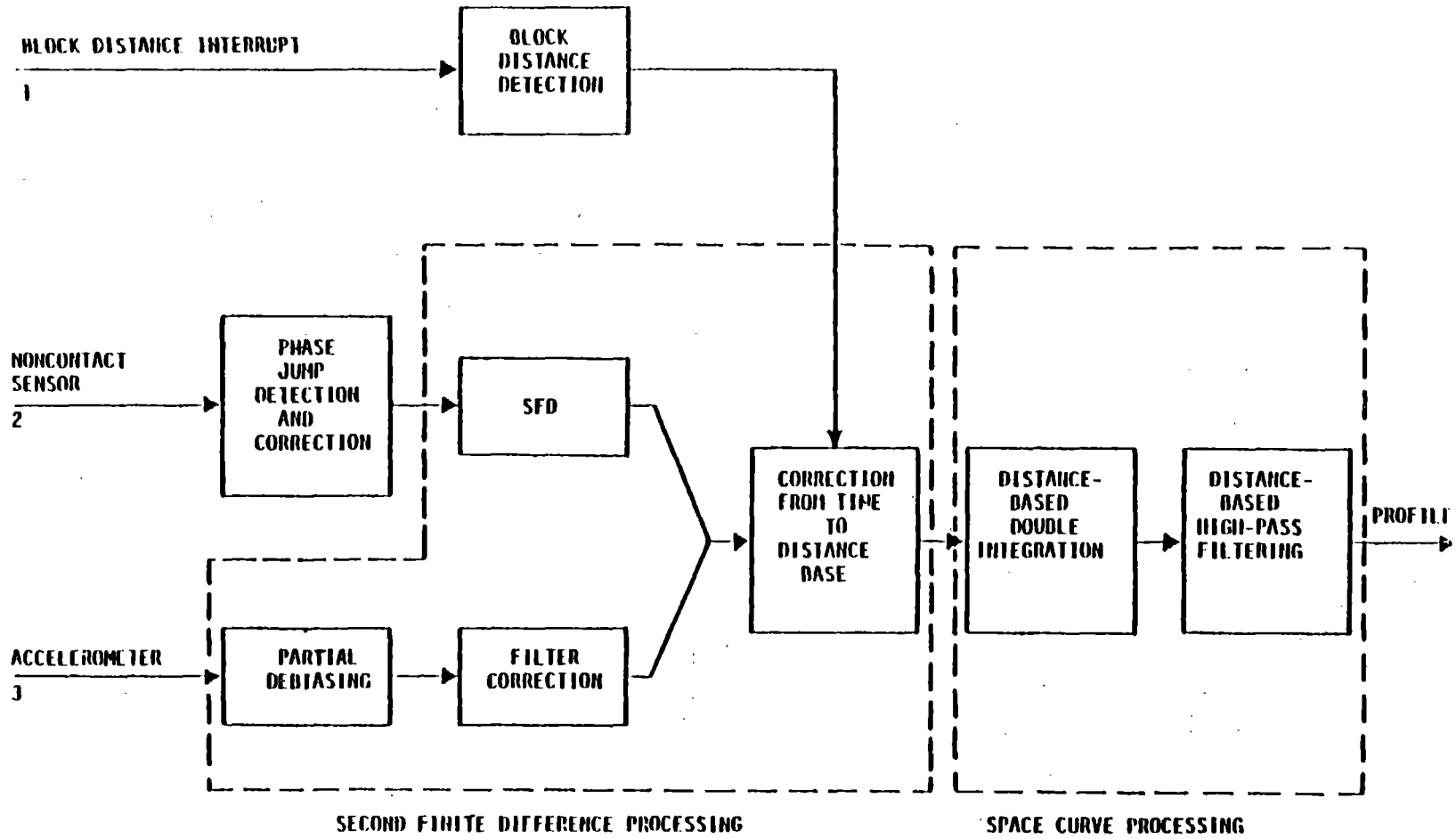


Figure 4. Conceptual Block Diagram of Digital Processing for Acoustic Probe Input (Displacement Input Mode).

Block Distance Processing

The desired output format of the road profile measurement is in vertical surface height variation as a function of distance along the direction of travel. The transducers used to perform the measurement (such as accelerometer and velocity transducer) and the signal conditioning electronics (such as filters and amplifiers) all have response characteristics which are functions of temporal frequency. As a result, measured road profile will be affected by vehicle speed if proper compensations are not made during the profile calculations. The basic scheme of the profile calculation used in the system samples the analog transducer signals at a constant time frequency of 4000Hz; a block distance data channel records pulses which are generated at fixed distance intervals by a wheel-driven tachometer. These distance-based pulses recorded on time-based sampling processes implicitly provide information on the speed of the vehicle. The software algorithms in the computer then take the time-based transducer data streams and use the distance pulses as a reference to compensate for the effect of speed and to convert the data to a distance-based format.

The block distance channel has a signal that is normally constant at +5 volts. When a block distance interrupt occurs, the signal drops to zero and then rises back to +5 volts, all occurring over an interval of approximately 0.5ms.

The block distance processing computes the first difference of this signal and compares it with a threshold value. On the first occasion that the threshold is exceeded in a given pulse, a logical variable, OFF, is set to false (OFF is true otherwise). The block distance subroutine, BLKDIS, contains logic that prevents more than one OFF=.FALSE. indication as the signal falls from +5 volts to zero and also prevents such indications as the signal rises back to +5 volts. Therefore, the beginning of a block distance interval is the first time step for which the

decrease in the signal exceeds a built-in threshold value. The threshold is normally set at about one-third of the equivalent of five volts.

3.0 PHASE JUMP PROCESSING

3.1 INTRODUCTION

The acoustic probe produces a phase angle output that is limited to a 0-360 degree range. This corresponds to a vertical displacement of approximately 0.8 inch (2cm). If the phase angle increases to 360 degrees, it then jumps back to zero and starts over. There is an opposite jump if the phase angle decreases to zero.

The current acoustic probe has an analog device called a range extender that detects the phase jumps and adds (or subtracts) the equivalent of 360 degrees so that the resulting signal is continuous and has a range of many times 360 degrees. The range extender is a complex piece of equipment that may not always perform properly. Also, when it corrects for a jump, it leaves a characteristic spike at that point in the output signal.

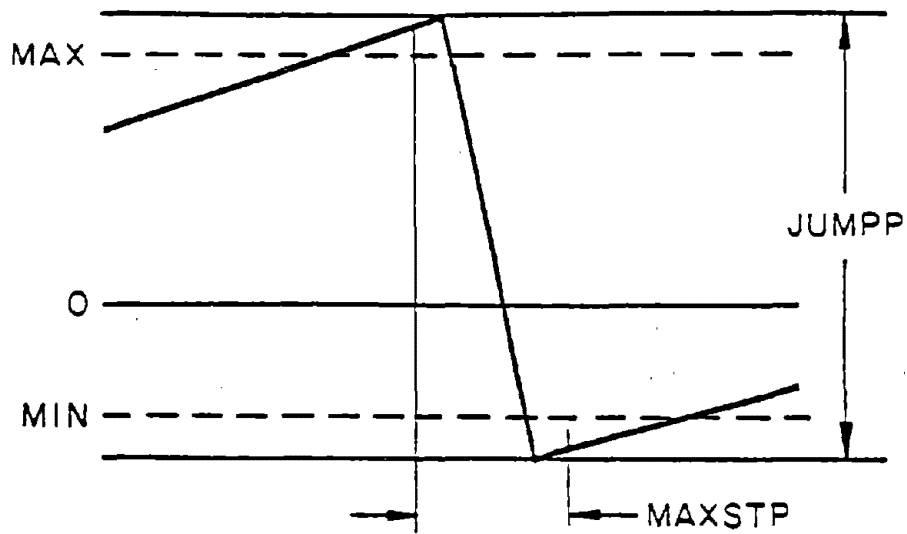
The phase jump processing is a digital replacement for the range extender. It detects phase jumps and corrects for them with greater reliability and smoothness than is possible with the range extender.

3.2 PHASE JUMP CHARACTERISTICS

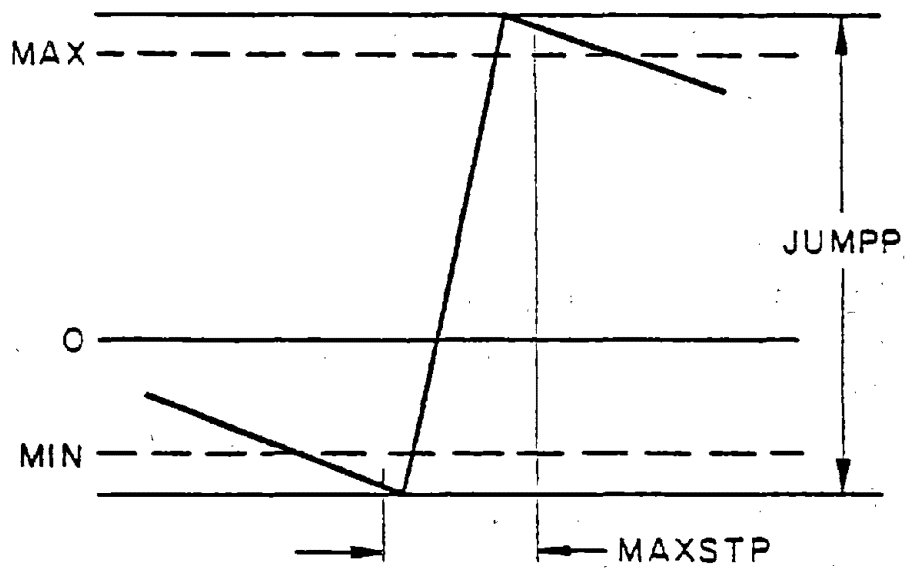
Two cases must be considered:

- Case 1 - the signal reaches a value close to the equivalent of 360 degrees and then jumps down close to the equivalent of zero degrees, and
- Case 2 - the signal reaches a value close to the equivalent of zero degrees and then jumps up close to the equivalent of 360 degrees.

These two cases are illustrated in Figure 5.



a) Case 1



b) Case 2

Figure 5. Characteristics of the Two Types of Phase Jumps.

Two thresholds, MIN and MAX, are indicated in the figure. They divide the total phase angle range into three regions: an upper region above MAX, a middle region between MAX and MIN, and a lower region below MIN. The characteristic feature of a phase jump is that the phase angle moves from the upper region to the lower region - or vice versa - in at most MAXSTP time steps. The size of MAXSTP is determined by the time response of the phase meter's jump circuitry, but MAXSTP is short enough to exclude any measured profile variations. (Even a jump in the pavement would be measured over an appreciable period because the acoustic probe takes an average reading over an area approximately the size of a tire patch.)

3.3 PHASE JUMP DETECTION

Whenever the phase angle leaves either the upper or the lower region, a counter is started. If the angle then reaches the opposite region within MAXSTP time steps, a phase jump has occurred. If MAXSTP time steps pass before the phase angle reaches the opposite region, there has not been a phase jump, and the counter is reset to zero.

3.4 PHASE JUMP CORRECTION

If a phase jump is detected, the current time step, which is the one at the end of the jump, and all previous steps back to the beginning of the jump need to be corrected. The current step is corrected by adding (or subtracting, as appropriate) JUMPP, which is the jump amplitude. At this point the steps at the beginning and end of the jump are correct. All steps in between are adjusted to yield a straight line between the beginning and end points.

It is necessary to introduce a delay into the data so that past time steps can be adjusted before they are used in further digital processing. The maximum delay needed is MAXSTP steps. To

preserve the relative timing between the data channels, all three channels (block distance, noncontact sensor and accelerometer) are delayed by MAXSTP time steps.

4.0 SECOND FINITE DIFFERENCE PROCESSING

4.1 INTRODUCTION

The so-called second finite difference (SFD) processing accomplishes the following:

- it corrects for the attenuation of the acceleration signal caused by the analog accelerometer filter,
- it corrects similarly for the analog filtering of the velocity signal if the noncontact sensor provides velocity information,
- it transforms displacement, velocity and acceleration signals to a common medium so that they can be combined,
- it combines the accelerometer and noncontact sensor signals into a single signal, and
- it converts the combined signal from time-based sampling to distance-based sampling.

For computational efficiency, the operations indicated above are not actually performed in the order indicated.

A common medium is needed which is conducive to combining displacement, velocity and acceleration data, to converting to distance-based sampling and ultimately to performing the double integration and high-pass filtering needed to obtain a road profile. The medium selected for all of these operations is the second finite difference of displacement.

The algorithms used in the SFD processing are developed in detail below.

4.2 GENERATION OF THE SFD

4.2.1 ACCELERATION SIGNAL

The digital input data includes an accelerometer signal processed

with the analog filter

$$H_a(s) = \frac{\omega_a^2}{s^2 + \omega_a s + \omega_a^2} \quad (23)$$

where s is the Laplace operator, ω_a is the filter corner frequency and subscript a denotes acceleration.

The digital processing includes a filter to compensate for the analog filtering. This filter can be obtained by inverting Equation (23) and replacing s with its sampled-data equivalent, $(1 - z^{-1})/T$, where T is the sample time and z is the sampled-data transform operator⁷. The result is

$$I_a(z) = \frac{1}{(\omega_a T)^2} \left[(1 - z^{-1})^2 + (1 - z^{-1})\omega_a T + (\omega_a T)^2 \right]. \quad (24)$$

The application of $I_a(z)$ to digital acceleration data produces a compensated digital acceleration. For further processing, however, it is preferable to work with the SFD of displacement rather than with acceleration. A displacement SFD can be obtained from a digital acceleration signal simply by multiplying by T^2 . The SFD form of Equation (24) then is

$$J_a(z) = \frac{1}{\omega_a^2 T^2} \left[(1 - z^{-1})^2 + (1 - z^{-1})\omega_a T + (\omega_a T)^2 \right] \quad (25)$$

⁷Z-transforms are described in the literature, for example in L. R. Rabiner and B. Gold, Theory and Application of Digital Signal Processing, Prentice-Hall, 1975. For present purposes it is sufficient to know that z^{-1} indicates a delay of one sample interval, so that $1 - z^{-1}$ is the finite difference operator.

This filter introduces an error in that there is a time shift among its three terms. The first term produces an SFD at T, the second term produces a first finite difference at T/2, and the third term has no time shift. To bring all of the terms into alignment and thus eliminate the error, they are all shifted to T:

$$K_a(z) = \frac{1}{\omega_a^2} \left[(1 - z^{-1})^2 + (1 - z^{-1})(1 + z^{-1})\frac{\omega_a T}{2} + (1 + z^{-1})^2 \left(\frac{\omega_a T}{2}\right)^2 \right]. \quad (26)$$

4.2.2 VELOCITY SIGNAL

Velocity input from the noncontact sensor also includes analog filtering, and it requires processing similar to the acceleration data:

$$H_V(s) = \frac{\omega_V}{s + \omega_V}, \quad (27)$$

$$J_V(z) = \frac{1}{\omega_V} \left[(1 - z^{-1}) + \omega_V T \right], \quad (28)$$

$$K_V(z) = \frac{1}{\omega_V} \left[(1 - z^{-1}) + (1 + z^{-1})\frac{\omega_V T}{2} \right]. \quad (29)$$

The processing technique calls for placing all of the input data in a form that is the SFD of displacement so that the

data channels can be combined so as to produce an SFD of the pavement profile. Toward this end, observe that $K_a(z)$ is the desired SFD due to the accelerometer input. For velocity input, an additional difference is required in order to obtain the SFD of displacement:

$$K'_v(z) = \frac{1}{\omega_v} \left[(1 - z^{-1})^2 + (1 - z^{-1})(1 + z^{-1}) \frac{\omega_v T}{2} \right]. \quad (30)$$

4.2.5 DISPLACEMENT SIGNAL

The displacement signal from the noncontact sensor requires no analog filtering, so the SFD form is obtained simply by performing two differencing operations on the input data:

$$K''_d(z) = (1 - z^{-1})^2. \quad (31)$$

4.3 CONVERSION TO DISTANCE-BASED SAMPLING

The next step is to convert from time-based SFD to a larger distance-based SFD. Let N be the number of time sample points occurring in a distance sample interval, $N \geq 1$. Observe that N may vary from one distance sample interval to the next. For the most part, variations in N will be accounted for automatically by the algorithm to be described. But occasionally a specific value of N will be needed, and then it will be necessary to have this value available for the specific distance interval of interest.

The conversion from time-based SFD to distance-based SFD is made with the following z -transfer function:

$$L(z) = \frac{(1 - z^{-N})^2}{(1 - z^{-1})^2}. \quad (32)$$

This transfer function is applied to Equation (26) for acceleration inputs, Equation (30) for velocity inputs, and Equation (31) for displacement inputs.

4.4 COMBINING THE ACCELEROMETER AND NONCONTACT SENSOR SIGNALS

The digitized accelerometer input data is denoted $\bar{a}(z)$ and is positive upward. The noncontact sensor input (displacement or velocity) is denoted $\bar{s}(z)$ and is positive when the pavement moves up relative to the vehicle. With these definitions, the pavement profile, $y(t)$, is

$$y(t) = \iint a(t) dt^2 + s(t) \quad (33)$$

for displacement input from the noncontact sensor or

$$y(t) = \iint a(t) dt^2 + \int s(t) dt \quad (34)$$

when the noncontact sensor provides velocity data.

To obtain the distance-based SFD of profile, $w(z)$, using displacement input, combine Equations (26), (31), (32) and (33).

$$\begin{aligned} w(z) &= \frac{(1 - z^{-N})^2}{(1 - z^{-1})^2} \left[K_a(z) \bar{a}(z) + K'_d(z) \bar{s}(z) \right] \\ &= (1 - z^{-N})^2 \left\{ \frac{1}{\omega_a^2} \left[1 + \frac{1 + z^{-1}}{1 - z^{-1}} \frac{\omega_a^T}{2} \right. \right. \\ &\quad \left. \left. + \frac{(1 + z^{-1})^2}{(1 - z^{-1})^2} \left(\frac{\omega_a^T}{2} \right)^2 \right] \bar{a}(z) + \bar{s}(z) \right\} \\ &= \frac{1}{\omega_a^2} (1 - z^{-N})^2 \left\{ \left[\bar{a}(z) + \omega_a^2 \bar{s}(z) \right] \right. \\ &\quad \left. + \frac{\omega_a^T}{2} \frac{1 + z^{-1}}{1 - z^{-1}} \bar{a}(z) + \left(\frac{\omega_a^T}{2} \right)^2 \frac{(1 + z^{-1})^2}{(1 - z^{-1})^2} \bar{a}(z) \right\} \quad (35) \end{aligned}$$

When the probe provides velocity data instead, then Equations (26), (30), (32) and (34) are combined similarly:

$$\begin{aligned}
 w(z) &= \frac{(1 - z^{-N})^2}{(1 - z^{-1})^2} \left[K_a(z) \bar{a}(z) + K'_v(z) \bar{s}(z) \right] \\
 &= \frac{1}{\omega_a^2} (1 - z^{-N})^2 \left\{ \left[\bar{a}(z) + \frac{\omega_a^2}{\omega_v} \bar{s}(z) \right] \right. \\
 &\quad \left. + \frac{\omega_a^T}{2} \frac{1 + z^{-1}}{1 - z^{-1}} \left[\bar{a}(z) + \omega_a \bar{s}(z) \right] \right. \\
 &\quad \left. + \left(\frac{\omega_a^T}{2} \right)^2 \frac{(1 + z^{-1})^2}{(1 - z^{-1})^2} \bar{a}(z) \right\} . \tag{36}
 \end{aligned}$$

Equations (35) and (36) can be combined by incorporating quantities ρ_1 and ρ_2 to distinguish between displacement and velocity input:

$$\rho_1 = \begin{cases} 1 & \text{for displacement input} \\ 1/\omega_v & \text{for velocity input} \end{cases} \tag{37}$$

and

$$\rho_2 = \begin{cases} 0 & \text{for displacement input} \\ \omega_a & \text{for velocity input.} \end{cases} \tag{38}$$

The combination of Equations (35) and (36) is then

$$\begin{aligned}
 w(z) = & \frac{1}{\omega_a^2} (1 - z^{-N})^2 \left\{ \left[\bar{a}(z) + \rho_1 \omega_a^2 \bar{s}(z) \right] \right. \\
 & + \frac{\omega_a^T}{2} \frac{1 + z^{-1}}{1 - z^{-1}} \left[\bar{a}(z) + \rho_2 \bar{s}(z) \right] \\
 & \left. + \left(\frac{\omega_a^T}{2} \right)^2 \frac{(1 + z^{-1})^2}{(1 - z^{-1})^2} \bar{a}(z) \right\} . \tag{39}
 \end{aligned}$$

4.5 COMPUTER IMPLEMENTATION

Equation (39) is in a form suitable for implementation on a digital computer. The computer program involves two nested loops. The inner loop does the time-based calculations and essentially performs the operations indicated inside the braces in Equation (39). The outer loop does the distance-based calculations, which is essentially the $(1 - z^{-N})^2$ operation in Equation (39).

4.5.1 INNER LOOP CALCULATIONS

The quantity

$$\bar{a}(z) + \rho_1 \omega_a^2 \bar{s}(z)$$

in Equation (39) requires no calculations in the inner loop.

The numerator of the quantity

$$\frac{1 + z^{-1}}{1 - z^{-1}} [\bar{a}(z) + \rho_2 \bar{s}(z)]$$

in Equation (39) is obtained by calculating

$$c + (a + a') + \rho_2(s + s') \quad (40)$$

where primes denote the corresponding quantity from the previous time step.⁸ The denominator, $1 - z^{-1}$, implies a single integration, which is obtained from

$$f + f + c. \quad (41)$$

The quantity

$$\frac{(1 + z^{-1})^2}{(1 - z^{-1})^2} \bar{a}(z)$$

in Equation (39) requires several calculations. First $(1 + z^{-1})\bar{a}(z)$ is obtained from

$$d + a + a' - 2b, \quad (42)$$

⁸ The symbol "+" means "assign the value of the quantity on the right to the variable on the left." It is written as an equals sign in FORTRAN, but has a different meaning than the algebraic equals sign [see Equation (41) for example].

where b is the bias in the acceleration signal, which can be calculated as indicated in Appendix A. Only for this particular quantity is it necessary to calculate and remove the bias. All other quantities that enter into $w(z)$ involve time-based first differences, $(1 - z^{-1})$, which effectively debias the SFD. This is apparent by examining Equations (26), (3) and (31).

The next step after Equation (42) is to calculate $(1 + z^{-1})^2 \bar{a}(z)$ using

$$e \leftarrow d + d'. \quad (43)$$

The denominator, $(1 - z^{-1})^2$, amounts to double integration. First and second integrals of e are obtained from

$$g \leftarrow g + e, \quad (44)$$

$$h \leftarrow H + g. \quad (45)$$

The last operation in the inner loop is to update a' , d' , s' and the inner loop index, n_1 :

$$a' \leftarrow a, \quad (46)$$

$$d' \leftarrow d, \quad (47)$$

$$s' \leftarrow s, \quad (48)$$

$$n_1 \leftarrow n_1 + 1. \quad (49)$$

4.5.2 OUTER LOOP CALCULATIONS

The inner loop (time-based) is continued until a block distance interrupt is encountered. At this point the current values of s , a , f , g , h and n_1 are used to perform the outer loop (distance-based) calculations. Inner loop values are transferred to outer loop values as follows:⁹

$$S \leftarrow s, \quad (50)$$

$$A \leftarrow a, \quad (51)$$

$$F \leftarrow f, \quad (52)$$

$$G \leftarrow g, \quad (53)$$

$$H \leftarrow h. \quad (54)$$

The quantity

$$(1 - z^{-N})^2 \left[\bar{a}(z) + \rho_1 \omega_a^2 \bar{s}(z) \right]$$

in Equation (39) is calculated using an SFD straightforwardly:

$$U \leftarrow S - S^*, \quad (55)$$

$$C \leftarrow A - A^* + \rho_1 \omega_a^2 U, \quad (56)$$

$$\Delta \leftarrow C - C^*. \quad (57)$$

where asterisks denote the corresponding quantity from the previous distance step.

The quantity

$$\frac{\omega_a^T}{2} (1 - z^{-N})^2 \frac{1 + z^{-1}}{1 - z^{-1}} \left[\bar{a}(z) + \rho_2 \bar{s}(z) \right]$$

⁹Quantity n_1 is a specific value of the more general quantity N . N does not appear explicitly in the outer loop calculations.

calls for an SFD involving F. Straightforward calculation would give

$$V + F - F^*, \quad (58)$$

$$\Delta + \Delta + \frac{\omega_a^T}{2} (V - V^*). \quad (59)$$

A simplification is possible, however. If we set $f = 0$ at the beginning of each distance-based loop, then at the end of the loop f will directly give a distance-based first finite difference. Then only the second difference need be calculated:

$$\Delta + \Delta + \frac{\omega_a^T}{2} (F - F^*). \quad (60)$$

The quantity

$$\left(\frac{\omega_a^T}{2}\right)^2 (1 - z^{-N})^2 \frac{(1 + z^{-1})^2}{(1 - z^{-1})^2} \bar{a}(z)$$

requires a somewhat more involved procedure. Straightforward calculation yields

$$Y + H - H^*, \quad (61)$$

$$\Delta + \Delta + \left(\frac{\omega_a^T}{2}\right)^2 (Y - Y^*). \quad (62)$$

Here again it is advantageous to set $h = 0$ at the beginning of outer loop. Then at the end of the loop h will directly give the distance-based first finite difference, and the calculation will be simplified as follows:

$$\Delta + \Delta + \left(\frac{\omega_a^T}{2}\right)^2 (H - H^*). \quad (63)$$

There is a more important reason for setting f and h to zero at the beginning of the outer loop. Examination of Equations (42) through (45) will reveal that h is a second integral of an acceleration measurement. Any uncompensated bias in a will cause h to grow quadratically. This error can be controlled by setting $h = 0$ periodically. Similarly, f is a first integral and can grow linearly with any bias in a , which motivates setting $f = 0$ at the beginning of the loop.

For the same reason, it is advisable to set $g = 0$ at the beginning of the outer loop. This, however, invalidates Equation (63) because the value of g that is discarded at the beginning of the outer loop should be integrated in the inner loop as a contributor to H [see Equations (45) and (54)]. Because the value of g that is discarded remains constant throughout the outer loop, its contribution to H is $n_1 G^*$, and the proper form of Equation (63) is

$$\Delta = \Delta + \left(\frac{\omega_a T}{2} \right)^2 (H + n_1 G^* - H^*). \quad (64)$$

Finally, the overall multiplier in Equation (39) is incorporated:

$$\Delta = \Delta / \omega_a^2. \quad (65)$$

The following quantities are updated at the end of the outer loop:

$$S^* = S, \quad (66)$$

$$A^* = A, \quad (67)$$

$$C^* = C, \quad (68)$$

$$F^* = F, \quad (69)$$

$$G^* = G, \quad (70)$$

$$H^* = H, \quad (71)$$

$$f = 0, \quad (72)$$

$$g = 0, \quad (73)$$

$$h = 0, \quad (74)$$

$$n_1 = 0. \quad (75)$$

5.0 SPACE CURVE PROCESSING

5.1 INTRODUCTION

The output of the SFD processing described in Section 4 is the SFD of the pavement profile. Space curve processing reduces the SFD to the profile itself.

The space curve algorithm basically provides double digital integration, and this part of the algorithm is quite simple. Double integration by itself, however, is unsatisfactory because various types of errors in the input signal or the initial conditions will cause the integrator output to grow without bound (see Section 1.2.1). Consequently, the space curve algorithm includes some rather elaborate high-pass filtering in order to remove the quantities that would otherwise cause unbounded growth of the output.

The filtering is accomplished by calculating an average of the data in the vicinity of the sample of interest. Then the average which is equivalent to low-pass filtering of the data, is subtracted from the sample of interest, which is equivalent to high-pass filtering of the sample of interest. This concept is described below.

5.2 FUNDAMENTALS OF FILTERING

5.2.1 FILTERING BY AVERAGING

Consider the data shown in Figure 6. These data apparently have considerable bias, which if double integrated, would give rise to quadratic growth of the output.

The bias can be removed by calculating an average of the data over an interval, say (x_a, x_b) and subtracting the average from the original data. If the average is denoted $\overline{x_{axb}}$, then

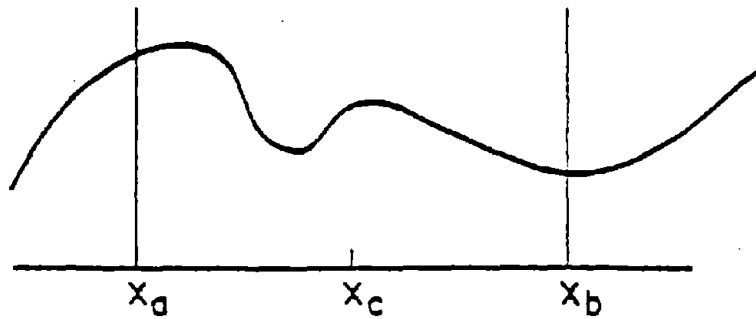


Figure 6. Typical Data

the debiased data is of the form $x_c - \overline{x_a x_b}$. Note that the removed bias is calculated within a "window" which moves with the point of interest, and, the bias calculated this way is generally not a fixed constant, rather, it follows the slow variations of the data stream.

The debiasing operation is a form of filtering that passes high frequencies and suppresses low frequency components. The cut-off frequency is inversely related to the averaging length, (x_a, x_b) .

It is important that x_c be located midway between x_a and x_b . This creates a (noncausal) symmetric filter that is direction invariant. A disadvantage of symmetric filters is that the output is delayed relative to the input. That is, the filtered value of x_c cannot be calculated until all data (x_a, x_b) are available. The delay involved, therefore, is one-half of the averaging length.

The example above involved continuous data, but the concepts carry over directly to sampled data. The averaging interval (x_a, x_b) should contain an odd number of samples so that the filter can be symmetric about a sample at the midpoint.

Consider a sequence of data f_i , $n_a \leq i \leq n_b$, with n_c being the midpoint. Then the average is

$$\bar{f}_{n_c} = \frac{1}{N} \sum_{i=n_a}^{n_b} f_i. \quad (76)$$

where

$$N = n_b - n_a + 1 \quad (77)$$

is the number of samples in the average (unrelated to N used in Section 4).

The filtered value of f_i is

$$f'_{n_c} = f_{n_c} - \bar{f}_{n_c}. \quad (78)$$

Quantities n_a , n_b and n_c are related as follows:

$$n_c = n_a + M = n_b - M, \quad (79)$$

$$M = \frac{N-1}{2}. \quad (80)$$

A convenient family of averaging lengths can be specified by use of the exponent n :

$$N = 2^n - 1. \quad (31)$$

Different values of n will provide different averaging length, therefore different cutoff frequency. The choice of the form $(2^n - 1)$ for the family of filter length is first to insure that the number of data points contained in the interval is odd and that the 2^n are the group of record sizes most convenient for computers to handle.

Computer implementation of the averaging could be done directly by use of Equation (76), but there is a more efficient method. Let

$$g_j = \sum_{i=j-M}^{j+M} f_i. \quad (83)$$

The advantage of this formulation is that it is related to the average through

$$\bar{f}_j = g_j/N \quad (85)$$

and it can be updated easily without calculation of the indicated sum:

$$g_j = g_{j-1} + f_{j+M} - f_{j-M-1}. \quad (84)$$

5.2.2 PROPERTIES OF AVERAGING FILTERS

Filters are often characterized by their impulse response or by its frequency-domain equivalent, frequency response. The impulse response¹⁰ of the averaging operation is a rectangular window with unit area, as shown in Figure 7.

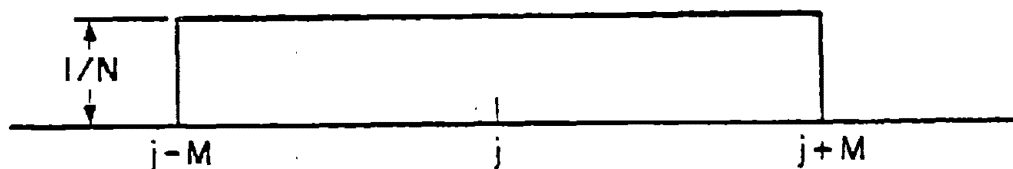


Figure 7. Impulse Response of Averaging

¹⁰ See, for example, pp. 13-14 of L.R. Rabiner and R. Gold, "Theory and Application of Digital Signal Processing", Prentice-Hall, Englewood Cliffs, New Jersey, 1975.

In the impulse response approach, averaging is done by convolving the data sequence, f_i , with the window in order to obtain the average $\overline{f_i}$. Debiasing is done by convolving the data with an impulse response function that combines a unit pulse with a negative unit rectangular window so that the net area under the function is zero. This is illustrated in Figure 8.

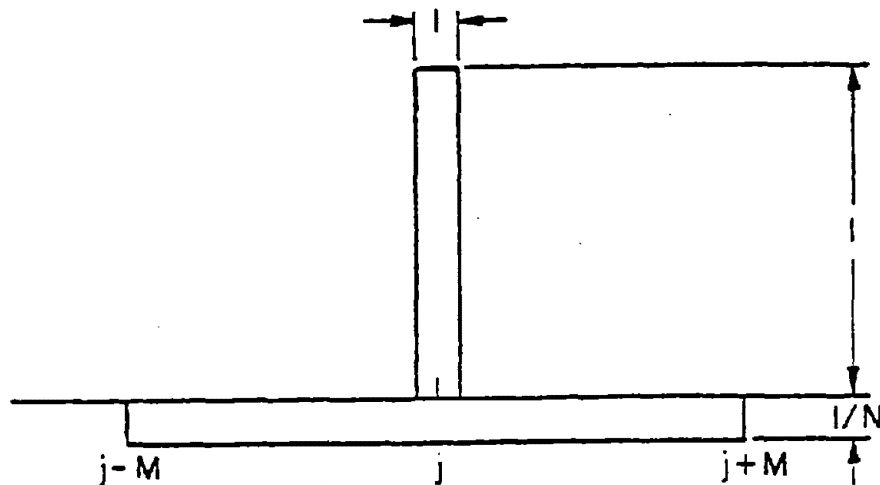


Figure 8. Impulse Response of Debiasing

The frequency response of the rectangular window (averaging) is¹¹

$$W(\phi) = \frac{\sin(N\pi\phi D)}{N \sin(\pi\phi D)} \quad (85)$$

where ϕ is the spatial frequency (cycles per unit distance) and D is the distance sampling interval. The debiasing operation has a frequency response

$$U(\phi) = 1 - W(\phi). \quad (86)$$

¹¹See Rabiner and Gold, pp. 90-91 for a derivation of the frequency response.

Both of these functions are plotted in Figure 9 versus the dimensionless frequency $\psi = N\phi D$.

It is clear that when ψ is used as the frequency instead of ϕ , the filter response amplitude is influenced only slightly by the value of N . The value of N also affects the upper frequency for which the filter should be used. This frequency is $\psi = N/2$, and it appears in Figure 9 for the $N = 7$ curve. For $\psi > N/2$, the frequency response "folds" over on itself so that the response curve has the same shape at $\psi = N$ as at $\psi = 0$. The value $\psi = N/2$ corresponds to $\phi = (2D)^{-1}$, that is, the maximum frequency that can be recovered for a given sampling rate.¹² Therefore, there is no need to use the filter beyond $\psi = N/2$.

5.2.3 HIGHER ORDER FILTERS

A shortcoming of the debiasing filter illustrated in Figure 9 is the ripple that occurs in its frequency response. This ripple can be reduced by using a higher order filter. For example, the filter

$$V(\phi) = 1 - W^3(\phi) \quad (87)$$

can be used. Its frequency response is illustrated in Figure 10. Overshoot for the higher order filter, $V(\phi)$, is only 1 percent compared with 22 percent for the simple filter, $U(\phi)$. The cutoff frequency is also lower for the higher order filter. As discussed later in this section, a W^5 -type filter is used in the final stage of the processing.

¹²See Rabiner and Gold, pp. 26-28, for further discussion of this problem.

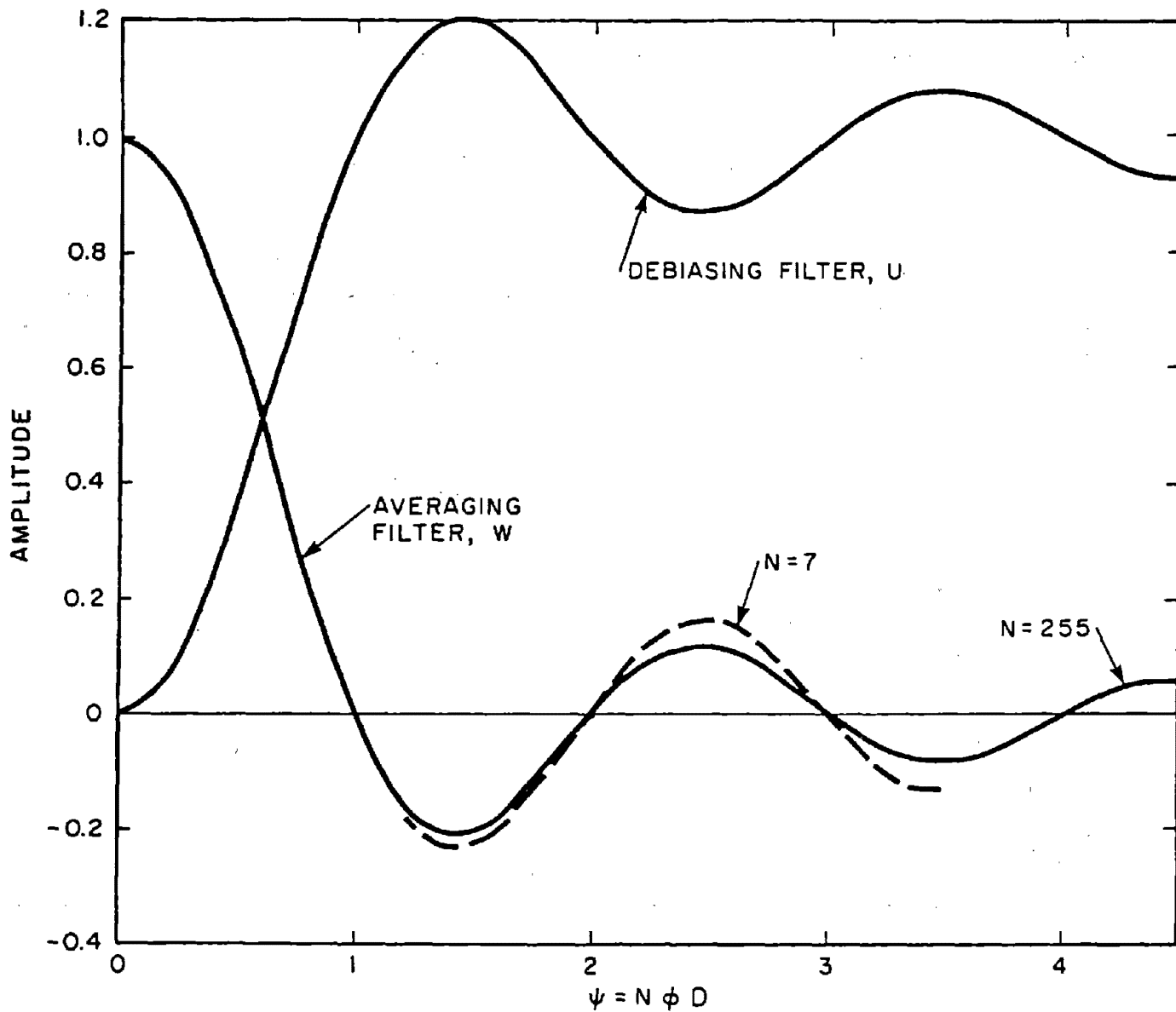


Figure 9. Frequency Response of Filters U and W.

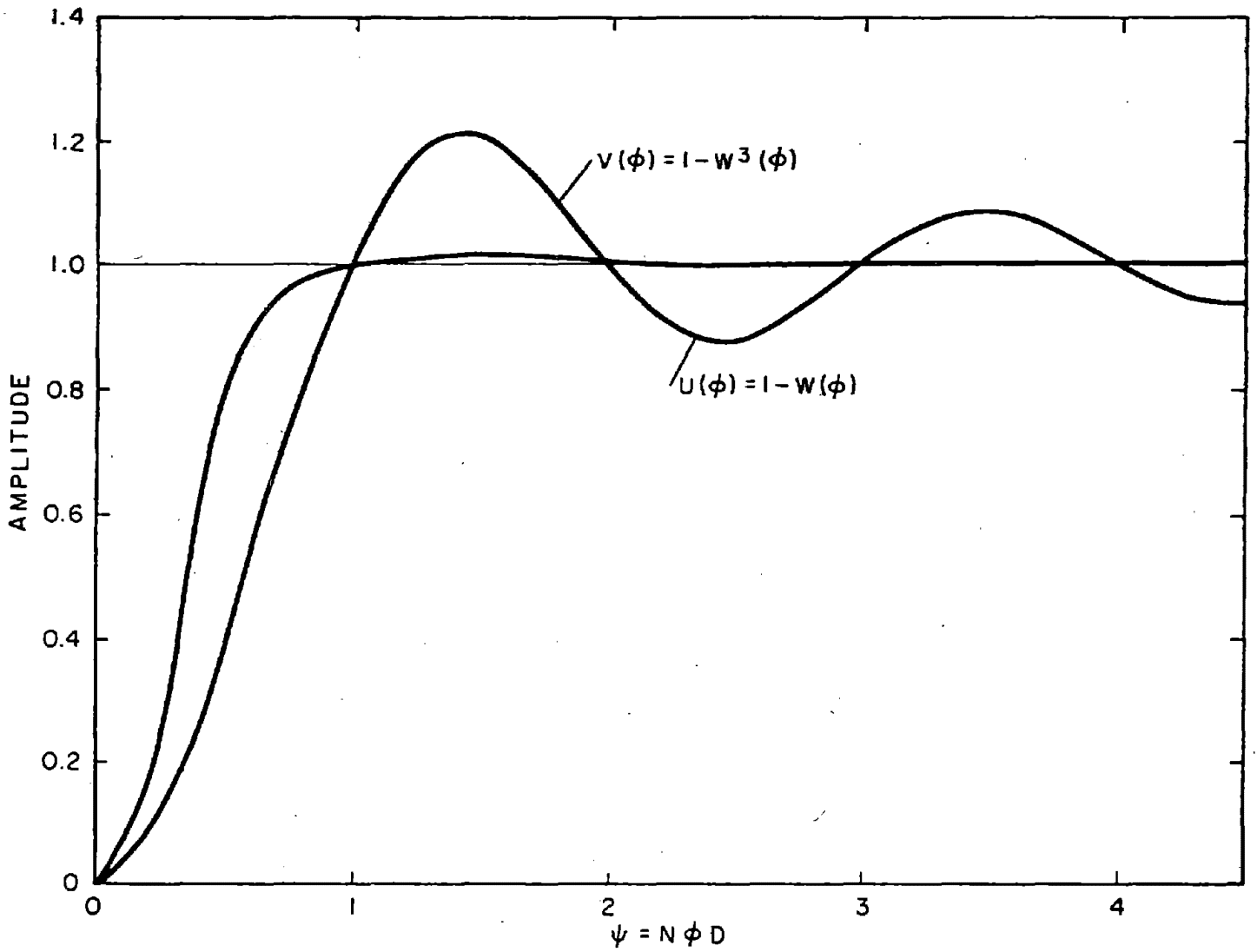


Figure 10. Frequency Response of Simple and Higher Order Filters ($N = 255$).

The ripple in $W(\phi)$ is associated with the discontinuity in its impulse response (see Figure 7). This is a well-known phenomenon.¹⁵

The impulse response associated with $W^3(\phi)$ is in fact smoother than that for $W(\phi)$. This smoother impulse response can be calculated by convolving a rectangular window with itself twice as shown in Figure 11.

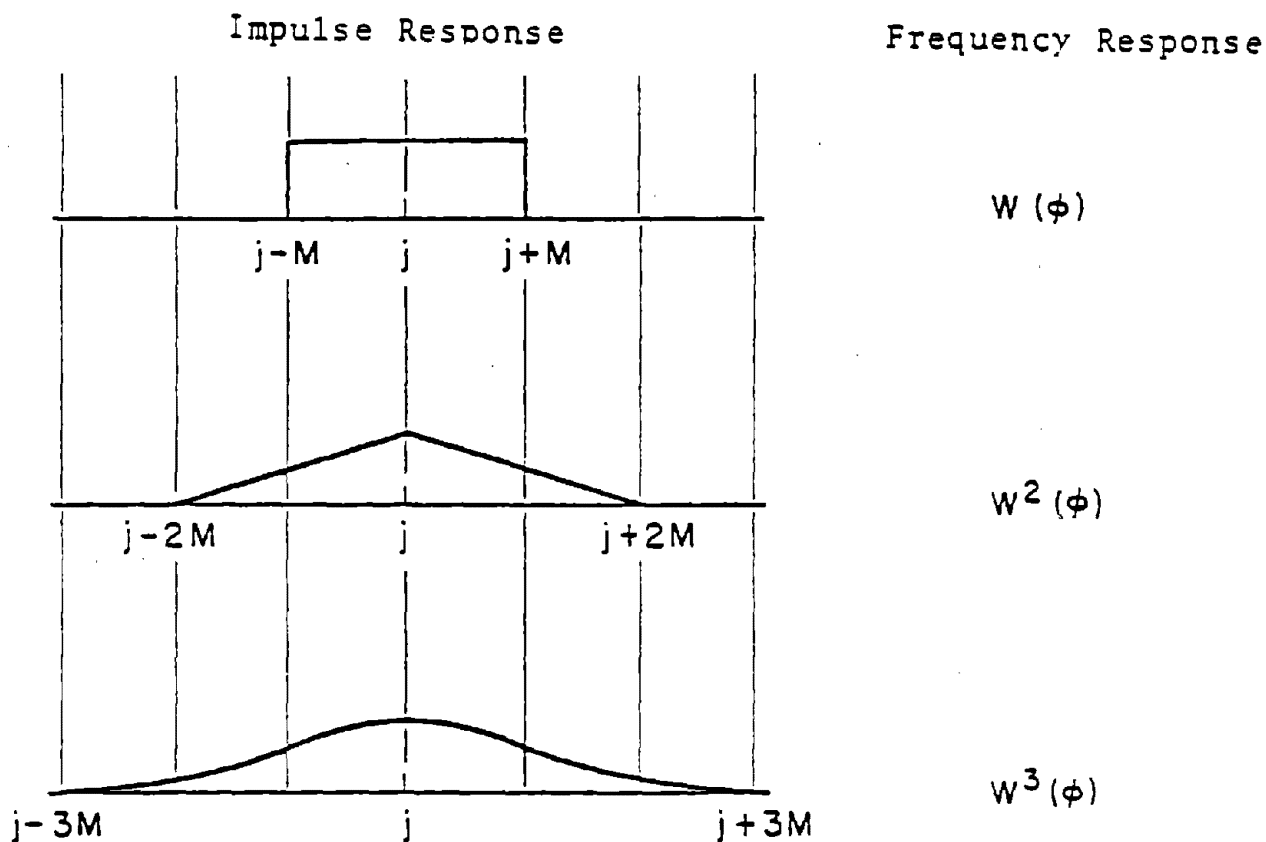


Figure 11. Response Comparison for Various Orders of Filters.

¹⁵See Rabiner and Gold, pp. 88-90, for further discussion.

In this figure the impulse response is a constant, linear or quadratic function, respectively, for the three cases shown.

Even higher orders of filtering can be obtained by obvious extension of the principles illustrated here. A $W^S(\phi)$ filter is used in the final stage of the space curve processing.

Computer implementation of higher order filters follows straightforwardly from the procedure described in Equations (83) and (84) for a simple filter. The simple filter provides a rectangular window, and to obtain the next order of filtering, one simply convolves this with another rectangular window, which is done by passing the output from Equations (83) and (84) through these same equations again:

$$g_j = g_{j-1} + \bar{f}_{j+M} - \bar{f}_{j-M-1}, \quad (84)$$

$$\bar{f}_j = g_j/N, \quad (83)$$

$$h_j = h_{j-1} + \bar{f}_{j+M} - \bar{f}_{j-M-1}, \quad (88)$$

$$\bar{f}_j = h_j/N. \quad (89)$$

This process can be thought of as "averaging the average." It produces a filter with frequency response $W^2(\phi)$, and the process can be repeated as many times as desired to obtain even higher order filters.

5.3 DOUBLE INTEGRATION

Integration is carried out on the computer with a simple summation operation:

$$q_j = q_{j-1} + p_j, \quad (90)$$

and double integration is accomplished by carrying out the same operation again:

$$r_j = r_{j-1} + q_j. \quad (91)$$

These integration formulas introduce a delay into the data. Quantity q_j actually represents the integral at a point midway between j and $j-1$. Therefore, a double integration introduces a delay of one sample in the data.

If the incoming data, p_j , includes a bias, Equation (90) will cause the bias to grow linearly, and Equation (91) will cause it to grow quadratically. In order to control errors, it is therefore essential to remove the bias in p_j with a debiasing filter. This filter should be of the type $V(\phi) = 1 - W^3(\phi)$ to reduce ripple. Direct implementation of $V(\phi)$ before integration could cause numerical problems, however, because the p_j data has a large dynamic range after passing through $V(\phi)$.

Consequently, an alternative approach is used. Quantity $V(\phi)$ is factored into

$$V(\phi) = 1 - W^3(\phi) = [1 - W(\phi)] [1 + W(\phi) + W^2(\phi)]. \quad (92)$$

This factorization is used to advantage by first passing the data through the $1 - W(\phi)$ filter (see Figure 8), which does

not introduce a large dynamic range, then by performing the double integration, and finally by passing the data through a $1 + W(\phi) + W^2(\phi)$ filter to reduce ripple. Figure 12 illustrates the impulse response of the data as it passes through these operations.

5.4 FINAL DEBIASING

Although the input data is debiased before further processing, the second integration operation introduces a bias into the impulse response (see Figure 12d). Thus, the output can still be biased. To eliminate this bias, a final debiasing operation is performed. This is done by generating a debiasing filter of the form $CW^m(\phi)$, where C and m are determined as discussed below.

Exponent m is chosen so that the debiasing term has ripple of the same order as the filter whose impulse response is shown in Figure 12g. From Figure 12 it can be seen that the tails of the impulse response are linear in Figure 12c, quadratic in Figure 12d, cubic in Figure 12e, and quartic in Figures 12f and 12g. Similar analysis of averaging filters as shown in Figure 11 reveals that a $W^5(\phi)$ filter is required to give quartic functions on the tails of the impulse response. Therefore, $m = 5$.

Coefficient C is calculated to give zero net area under the debiased impulse response. That is, C is such that the area under the impulse response corresponding to $CW^5(\phi)$ is equal to the area under Figure 12g. In order to calculate these areas, use is made of the averaging filter's property of preserving the area under the impulse response. This property

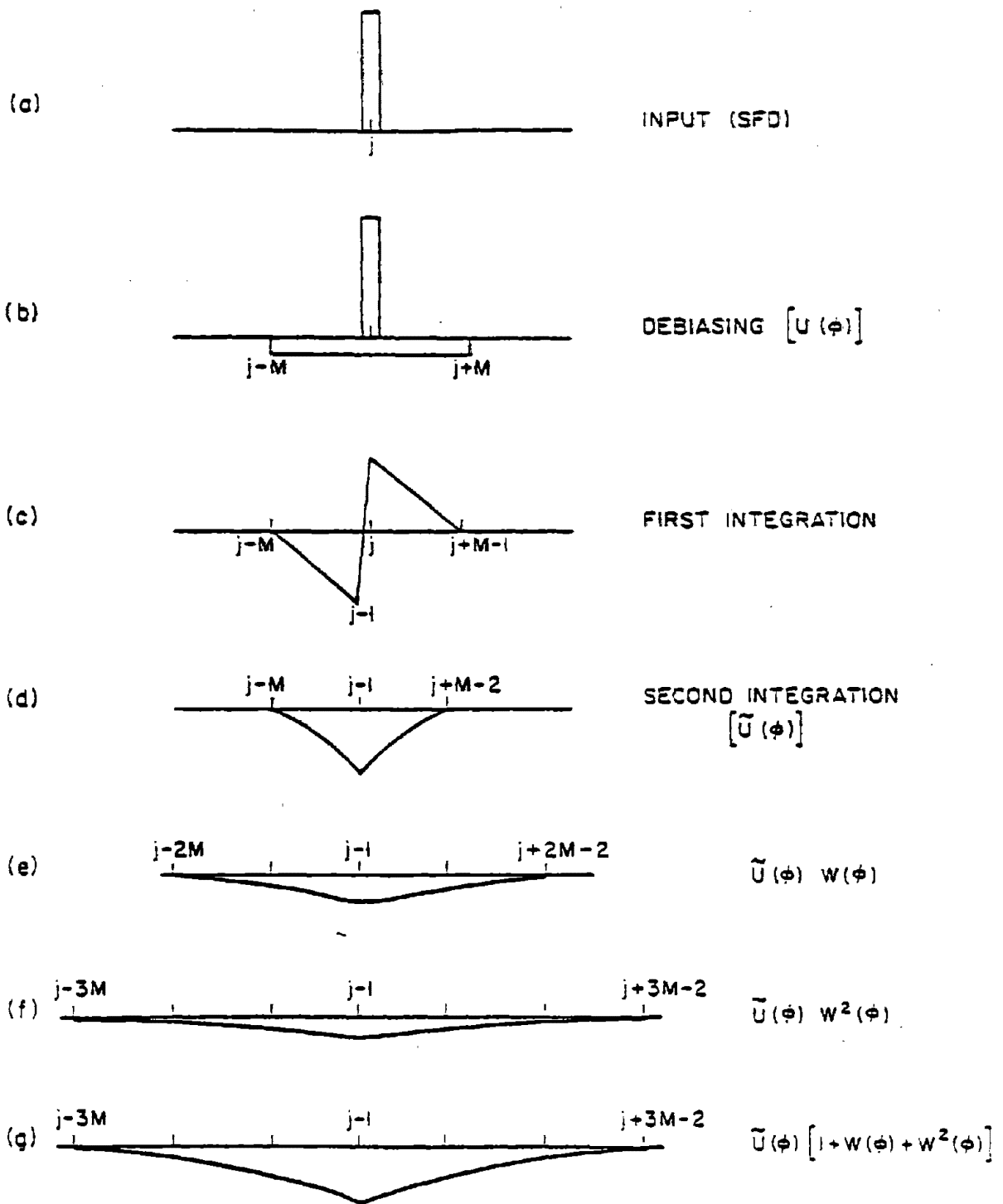


Figure 12. Impulse Responses for Filtering and Integration Operations.

follows from the facts that (1) this filter has unit impulse response and (2) any response is a superposition of impulse responses. It follows that the area under the impulse response corresponding to $W^5(\phi)$ is unity.

To calculate the area under Figure 12g, we first calculate the area under Figure 12d. Start with Figure 12b, and introduce index i such that $i = 1$ corresponds to $j = M$ in the figure. The ordinate in Figure 12b can be represented as

$$s_0(i) = -1/N, \quad i = 1, \dots, M. \quad (93)$$

The ordinate in Figure 12c is the integral of this:

$$\begin{aligned} s_1(i) &= \sum_{j=1}^i s_0(j) \\ &= -i/N. \end{aligned} \quad (94)$$

Another integration is used to obtain the ordinate in Figure 12d:

$$\begin{aligned} s_2(i) &= \sum_{j=1}^i s_1(j) \\ &= -\frac{i(i+1)}{2N} \end{aligned} \quad (95)$$

Because of symmetry, the total area under Figure 12d, S , is the ordinate of the midpoint, $s_2(M)$, plus twice the sum up to the midpoint:

$$\begin{aligned}
S &= 2 \sum_{i=1}^{M-1} s_2(i) + s_2(M) \\
&= \frac{-1}{N} \left[\sum_{i=1}^{M-1} i^2 + \sum_{i=1}^{M-1} i + \frac{M(M+1)}{2} \right] \\
&= \frac{-1}{N} \left[\frac{(M-1)M(2M-1)}{6} + \frac{(M-1)M}{2} + \frac{M(M+1)}{2} \right] \\
&= \frac{-(N^2-1)}{24} \tag{96}
\end{aligned}$$

where the identity $N = 2M+1$ is used.

Figures 12e and 12f represent averaging operations on Figure 12d, and thus they each have area S . Figure 12g is the sum of Figures 12d, 12e and 12f, so that the area under Figure 12g is $3S$. Therefore

$$C = 3S = \frac{-(N^2-1)}{8} \tag{97}$$

Figure 13 illustrates the impulse responses of Figure 12g before and after debiasing. In this figure the debiasing term is negative because C is negative, and the debiasing term is subtracted from the data in order to obtain the debiased result.

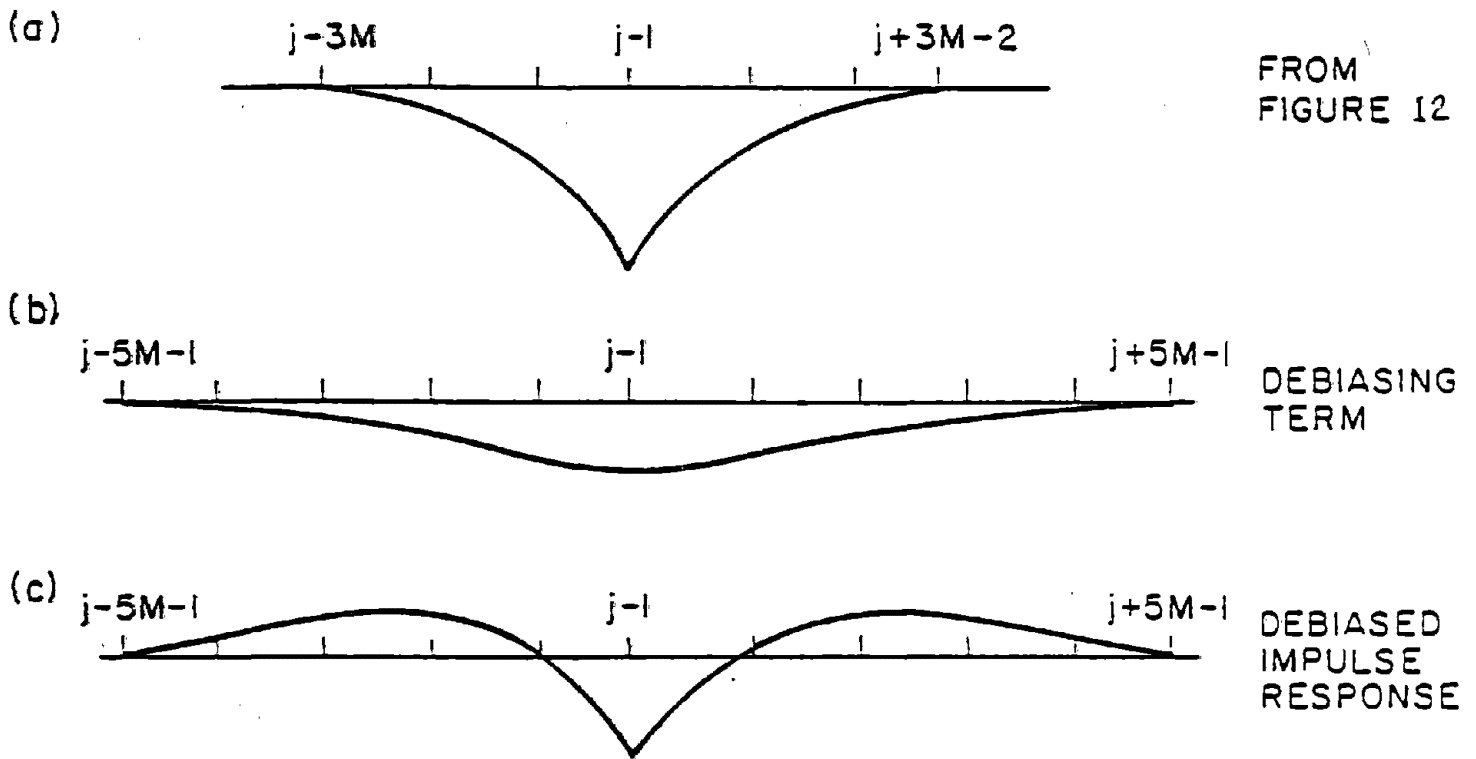


Figure 13. Impulse Responses for the Final Debiasing.

5.4.1 FINAL FREQUENCY RESPONSE

Figure 10 shows the frequency response for the filtering but not the integration operations in Figure 12. Because double integration is required in order to recover the space curve from the SFD, it is appropriate that only the filtering be included in the frequency response so that the frequency response characteristic portrays the filtering done to the output space curve by the processing. The debiasing term, $W^5(\phi)$, is not subject to

integration, however, so it is necessary to calculate the frequency response due to double integration and divide it out of the debiasing term in order to completely represent the filtering done to the output space curve.

To obtain the frequency response due to integration, the z-transform corresponding to Equation (90) is written,

$$\frac{1}{1-z^{-1}},$$

and the substitution

$$z = e^{j\theta}, \theta = 2\pi\phi D, \tag{98}$$

is made. The resulting quantity when squared,

$$\left(\frac{1}{1-e^{-j\theta}} \right)^2,$$

is the complex frequency response of double integration. To obtain the amplitude response, set

$$Y^*(\theta) = (1 - e^{-j\theta})^2 \tag{99}$$

and calculate

$$\begin{aligned} |Y^*(\theta)| &= (1 - \cos\theta)^2 + \sin^2 \theta \\ &= 2(1 - \cos\theta) \\ &= 4 \sin^2 \frac{\theta}{2}. \end{aligned} \tag{100}$$

Therefore, the amplitude response for double integration is

$$Y(\phi) = \frac{1}{4 \sin^2(\pi\phi D)}. \quad (101)$$

The debiased frequency response is obtained by adding¹⁴ the debiasing filter - divided by the frequency response of integration - to $V(\phi)$:

$$\begin{aligned} Z(\phi) &= 1 - W^3(\phi) + CW^5(\phi)/Y(\phi) \\ &= 1 - W^3(\phi) - \frac{N^2-1}{2} \sin^2(\pi\phi D) W^5(\phi) \end{aligned} \quad (102)$$

where $W(\phi)$ is given by Equation (85).

This function is plotted in Figure 14 along with the biased frequency response, $V(\phi)$. It can be seen that $Z(\phi)$ has a higher cutoff frequency and more overshoot than $V(\phi)$.

¹⁴ Investigation of the phase response associated with $Y(\phi)$ will reveal that the phase is approximately π radians in the frequencies of interest. [As discussed in connection with Figure 9, the maximum frequencies recoverable are such that $\phi D < 1/2$. For such frequencies one can see that the imaginary term dominates in Equation (100).] Therefore, double integration introduces a change of sign in the frequency response, and it is necessary to add rather than subtract the debiasing term in order to incorporate this sign change.

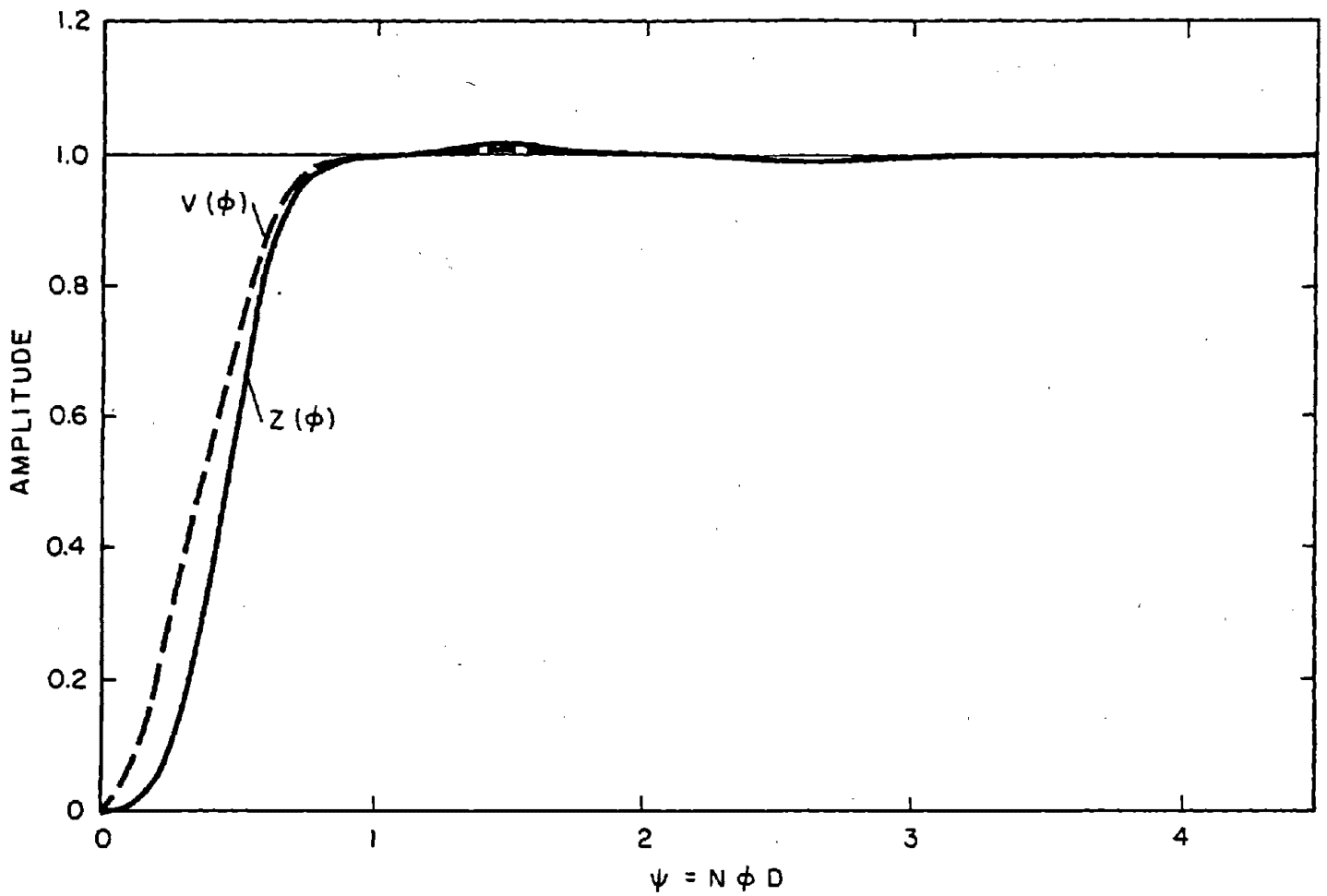


Figure 14. Frequency Response With and Without Debiasing (N = 255).

Table 1 gives the pertinent characteristics of $V(\phi)$ and $Z(\phi)$ (wavelength, $\lambda = 1/\phi$).

TABLE 1
 FREQUENCY RESPONSE CHARACTERISTICS OF
 SPACE CURVE FILTERING

	<u>$V(\phi)$</u> <u>$N = 255$</u>	<u>$Z(\phi)$</u> <u>$N = 255$</u>	<u>$Z(\phi)$</u> <u>$N = 31$</u>
Maximum Overshoot	1.01%	1.52%	1.53%
Wavelength for 0.90 Amplitude Response	1.588ND	1.506ND	1.505ND
Wavelength for $1/\sqrt{2}$ Amplitude Response	2.091ND	1.843ND	1.842ND

Table 2 is calculated using an average $1/\sqrt{2}$ cutoff for $Z(\phi)$. This table shows how N and D must be selected to provide the desired filter cutoff for a particular application.

TABLE 2
 SPACE CURVE CUTOFF WAVELENGTH (In Feet)

<u>Sampling Interval</u>	<u>$N = 31$</u>	<u>$N = 63$</u>	<u>$N = 127$</u>	<u>$N = 255$</u>
1 inch	4.8	9.7	19.5	39.1
2 inches	9.5	19.3	39.0	78.3
4 inches	19.0	38.7	78.0	157
8 inches	38.1	77.4	156	313

5.5 AN EXAMPLE

All of the information needed to understand the space curve algorithm is provided above, but to make it clearer just how all of the pieces fit together, a comprehensive example is provided here. The example is the calculation of the impulse response as portrayed in Figure 13c using $N = 7$ (this is the smallest value of N that illustrates all of the principles involved). Accordingly, the input sequence is the value "1" preceeded and followed by infinitely many zeros.

Table 3 displays the calculations involved in processing the input sequence. Each row in the table represents one pass through the algorithm, that is, one call to the space curve subroutine. The columns in the table represent specific parts of the algorithm. The column headings include the column number, the type of computational operation performed, the columns from which the data is drawn, and the associated variables in the computer program. The columns relate to the preceding figures as follows:

Column	Figure
1	12a
-	12b
8	12c
9	12d
11	12e
12	12f
13	12g, 13a
14	13b
15	13c

It is apparent that each column in the table is symmetric about some midpoint. The midpoint for the input data is step 1, and for the output it is step 16, which represents a delay

TABLE 3
CALCULATION OF SPACE CURVE IMPULSE RESPONSE FOR N = 7

COLUMN	1	2	3	4	5	6	7	8	9	10	11	12	13	14	15
OPERATION	INPUT	FIRST AVERAGE	SECOND AVERAGE	THIRD AVERAGE	FOURTH AVERAGE	FIFTH AVERAGE	DELAY INPUT	DEBIAS & LST INTEGRAL	SECOND INTEGRAL	N-SAMPLE DELAY	AVERAGE INTEGRATOR OUTPUT	SECOND AVERAGE	COMBINE HIGHER ORDER TERMS	DEBIAS TERM	DEBIASED OUTPUT
DATA FROM COLUMNS	-	1	2	3	4	5	1	2,7	8	9	10	11	10,11,12	6	13,14
VARIABLES IN THE CODE	DELTA AVG (1,*)	XX(1) AVG (2,*)	XX(2) AVG (3,*)	XX(3) AVG (4,*)	XX(4) AVG (5,*)	XX(5) BIAS	X	XL0	XL1	SPCURV(1,*) X SPCURV(2,*)	XX(6),X SPCURV(3,*)	XX(7) XX(7) X	X	XX	SPC
STEP 1	1	1/7	1/7 ²	1/7 ³	1/7 ⁴	1/7 ⁵	0	-1/7	-1/7	0	0	0	0	-6/7 ⁵	6/7 ⁵
2	0	1/7	2/7 ²	3/7 ³	4/7 ⁴	5/7 ⁵	0	-2/7	-3/7	0	0	0	0	-30/7 ⁵	30/7 ⁵
3	0	1/7	3/7 ²	6/7 ³	10/7 ⁴	15/7 ⁵	0	-3/7	-6/7	0	0	0	0	-90/7 ⁵	90/7 ⁵
4	0	1/7	4/7 ²	10/7 ³	20/7 ⁴	35/7 ⁵	1	3/7	-3/7	0	0	0	0	-210/7 ⁵	210/7 ⁵
5	0	1/7	5/7 ²	15/7 ³	35/7 ⁴	70/7 ⁵	0	2/7	-1/7	0	0	0	0	-420/7 ⁵	420/7 ⁵
6	0	1/7	6/7 ²	21/7 ³	56/7 ⁴	126/7 ⁵	0	1/7	0	0	0	0	0	-756/7 ⁵	756/7 ⁵
7	0	1/7	7/7 ²	28/7 ³	84/7 ⁴	210/7 ⁵	0	0	0	0	0	0	0	-1260/7 ⁵	1260/7 ⁵
8	0	0	6/7 ²	33/7 ³	116/7 ⁴	325/7 ⁵	0	0	0	-1/7	-1/7 ²	-1/7 ³	-1/7 ³	-1950/7 ⁵	1901/7 ⁵
9	0	0	5/7 ²	36/7 ³	149/7 ⁴	470/7 ⁵	0	0	0	-3/7	-4/7 ²	-5/7 ³	-5/7 ³	-2820/7 ⁵	2575/7 ⁵
10	0	0	4/7 ²	37/7 ³	180/7 ⁴	640/7 ⁵	0	0	0	-6/7	-10/7 ²	-15/7 ³	-15/7 ³	-3804/7 ⁵	3105/7 ⁵
11	0	0	3/7 ²	36/7 ³	206/7 ⁴	826/7 ⁵	0	0	0	-3/7	-13/7 ²	-28/7 ³	-35/7 ³	-4956/7 ⁵	3241/7 ⁵
12	0	0	2/7 ²	33/7 ³	224/7 ⁴	1015/7 ⁵	0	0	0	-1/7	-14/7 ²	-42/7 ³	-70/7 ³	-6090/7 ⁵	2660/7 ⁵
13	0	0	1/7 ²	28/7 ³	231/7 ⁴	1190/7 ⁵	0	0	0	0	-14/7 ²	-56/7 ³	-126/7 ³	-7140/7 ⁵	966/7 ⁵
14	0	0	0	21/7 ³	224/7 ⁴	1330/7 ⁵	0	0	0	0	-14/7 ²	-70/7 ³	-210/7 ³	-7980/7 ⁵	-2310/7 ⁵
15	0	0	0	15/7 ³	206/7 ⁴	1420/7 ⁵	0	0	0	0	-13/7 ²	-82/7 ³	-327/7 ³	-8520/7 ⁵	-7503/7 ⁵
16	0	0	0	10/7 ³	180/7 ⁴	1451/7 ⁵	0	0	0	0	-10/7 ²	-88/7 ³	-480/7 ³	-8706/7 ⁵	-1418/7 ⁵
17	0	0	0	6/7 ³	149/7 ⁴	1420/7 ⁵	0	0	0	0	-4/7 ²	-82/7 ³	-327/7 ³	-8520/7 ⁵	-7503/7 ⁵
18	0	0	0	1/7 ³	116/7 ⁴	1330/7 ⁵	0	0	0	0	-1/7 ²	-70/7 ³	-210/7 ³	-7980/7 ⁵	-2310/7 ³
19	0	0	0	1/7 ³	84/7 ⁴	1190/7 ⁵	0	0	0	0	0	-56/7 ³	-126/7 ³	-7140/7 ⁵	996/7 ⁵
20	0	0	0	0	56/7 ⁴	1015/7 ⁵	0	0	0	0	0	-42/7 ³	-70/7 ³	-6090/7 ⁵	2660/7 ⁵
21	0	0	0	0	35/7 ⁴	826/7 ⁵	0	0	0	0	0	-28/7 ³	-35/7 ³	-4956/7 ⁵	3241/7 ⁵
22	0	0	0	0	20/7 ⁴	640/7 ⁵	0	0	0	0	0	-15/7 ³	-15/7 ³	-3840/7 ⁵	3105/7 ⁵
23	0	0	0	0	10/7 ⁴	470/7 ⁵	0	0	0	0	0	-5/7 ³	-5/7 ³	-2820/7 ⁵	2575/7 ⁵
24	0	0	0	0	4/7 ⁴	325/7 ⁵	0	0	0	0	0	-1/7 ³	-1/7 ³	-1950/7 ⁵	1901/7 ⁵
25	0	0	0	0	1/7 ⁴	210/7 ⁵	0	0	0	0	0	0	0	-1260/7 ⁵	1260/7 ⁵
26	0	0	0	0	0	126/7 ⁵	0	0	0	0	0	0	0	-756/7 ⁵	756/7 ⁵
27	0	0	0	0	0	70/7 ⁵	0	0	0	0	0	0	0	-420/7 ⁵	420/7 ⁵
28	0	0	0	0	0	35/7 ⁵	0	0	0	0	0	0	0	-210/7 ⁵	210/7 ⁵
29	0	0	0	0	0	15/7 ⁵	0	0	0	0	0	0	0	-90/7 ⁵	90/7 ⁵
30	0	0	0	0	0	5/7 ⁵	0	0	0	0	0	0	0	-30/7 ⁵	30/7 ⁵
31	0	0	0	0	0	1/7 ⁵	0	0	0	0	0	0	0	-6/7 ⁵	6/7 ⁵
TOTALS	1	1	1	1	1	1	1	0	-2	-2	-2	-2	-6	-6	0

of 15 steps (5M steps in general). The overall length of the filter is determined by the fifth average, which is 31 steps long (10M + 1 in general). The columns do not all have the same midpoints, as opposed to the aligned illustrations in the figures, and thus it is necessary to introduce delays into the algorithm at appropriate points to bring all terms into proper alignment.

Totals are provided for all values in each column. These totals are helpful in understanding the calculation of the debiasing coefficient. The column 15 total shows that the net area under the impulse response is zero, and thus any biases in the data or the processing are cancelled from the output.

5.6 REAL TIME IMPLEMENTATION OF THE ALGORITHM

Although the algorithm described above is suitable for real time implementation, further analysis is needed to render the algorithm into a form that is properly scaled, reasonably free from numerical problems, and as efficient as possible.

As an illustration of what can be done to improve efficiency, consider the large number of divisions by N that are required (columns 2, 3, 4, 5, 6, 8, 11, 12 in Table 3). In machine language, division by N can be done by a simple shift operation if $N = 2^n$. In our case $N = 2^n - 1$, however, so adjustments are necessary to take advantage of division by shifting. This is done by dividing by 2^n and then correcting at the end of the algorithm with the factor

$$\frac{2^n}{2^n - 1} = \frac{1}{1 - 2^{-n}} = 1 + 2^{-n} . \quad (103)$$

For the debiasing term, which involves five such divisions, for example, the correction factor is

$$(1 + 2^{-n})^5 = 1 + 5 \cdot 2^{-n}. \quad (104)$$

6.0 THE COMPUTER PROGRAM

The digital processing algorithms described in Sections 2-5 are implemented in a computer program written in ANSI FORTRAN IV. This section describes the details of this program for offline processing.

6.1 PROGRAM STRUCTURE AND SUBROUTINES

6.1.1 OVERALL STRUCTURE

The program comprises a main program and five subroutines, all of which are called by the main program. The main program reads the input data, sets up processing constants, provides overall control of the processing, and calls the five subroutines to handle specific parts of the processing. The main program is discussed in detail in Section 6.1.2, and the subroutines are described below.

Subroutine BLKDIS. This subroutine processes the input (time-based) block distance signal to detect the distance-based block distance interrupts. Its output is the logical variable OFF, which is normally true but is false if there is a block distance interrupt. Variable OFF is used by subroutine SFD to trigger the time-to-distance conversion. The algorithm used in BLKDIS is described in Section 2.2.2.

Subroutine JUMP. This subroutine detects and eliminates phase jumps in the acoustic probe signal. In so doing, it introduces a small delay (currently 12 time scans) into all three input data channels. The algorithm used is described in Section 3.

Subroutine SFD. This subroutine corrects for the acceleration and velocity analog filters, combines the accelerometer and non-contact sensor signals, and converts from time-based to distance-

based sampling. The inputs are the accelerometer and noncontact sensor signals obtained from JUMP and the block distance trigger OFF, obtained from BLKDIS. The output is the SFD of profile. Section 4 describes the algorithm employed.

Subroutine SPACEC. This subroutine performs the double integration required to reduce the SFD to pavement profile and also introduces high-pass distance-based filtering to control error and suppress undesired long wavelength terrain components. The input is the distance-based SFD obtained from subroutine SFD, and the output is the desired distance-based pavement profile. The algorithm is described in Section 5.

Subroutine OUTPUT. This simple subroutine collects output from five channels scan-by-scan until 256 distance-based scans are accumulated and then writes the resulting record on the desired output unit. It also fills the end of the last output record with zeros as needed so that it has 256 scans and no data are lost at the end of the run. The method used is evident from the source listing in Appendix B.

6.1.2 MAIN PROGRAM

Overview

The main program first reads a header record that identifies the data being processed. Then two records of run parameters are read. Certain processing constants dependent on the run parameters are calculated. Next, the file of digitized input data is positioned at the desired starting record as specified by the run parameters. The header and run parameters are written on unit 6 to provide a written record of the run.

The program then enters the main processing loop, which indexes over the specified number of records of time-based digitized input

data. Inside this loop is another loop, which indexes over the 256 time-based scans within each input record.

Within the inner loop, JUMP is called to do the phase jump processing; BLKDIS is called to determine if the present time-based scan is also the end of a distance-based scan (OFF=.FALSE.); subroutine SFD is called to handle the SFD processing; and if OFF=.FALSE., then SPACEC and OUTPUT are called to do the distance-based processing and save the results, respectively.

When the outer loop has exhausted the specified input records, the program generates an additional input record that corresponds to perfectly flat pavement at the height of the last processed input scan. This record is processed as many times as is necessary to flush out the output profile value corresponding to the last input data. (The delay imposed by the space curve filter necessitates the flushing if the last value is desired.) Variables IEOF and IEXTRA control the amount of extra processing needed. Variables MSTEP and NSTEP generate uniform block distance interrupts at a rate corresponding to the last of the input data.

When the flushing is complete, OUTPUT is called one more time so that it can fill out the current output record with zeros and transfer the record to the output file.

Finally, the number of input and output records processed is written on unit 6 and the files are closed.

Flowchart

A flowchart of the main program is provided in Figure 15.

6.2 INPUT DATA

The input is in two forms, the run parameters, which are read from unit 5, and the data to be processed, which are read from

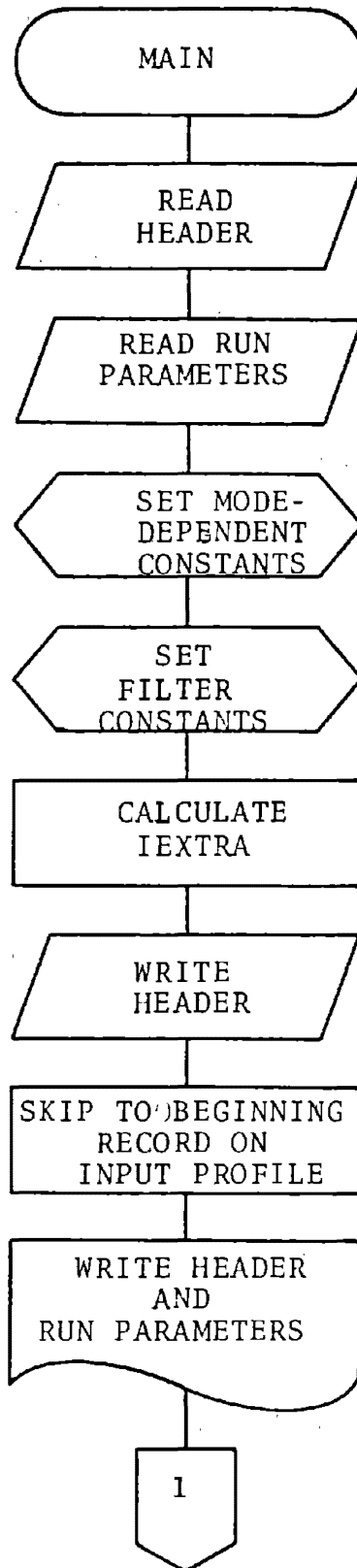


Figure 15. Flowchart of Main Program.

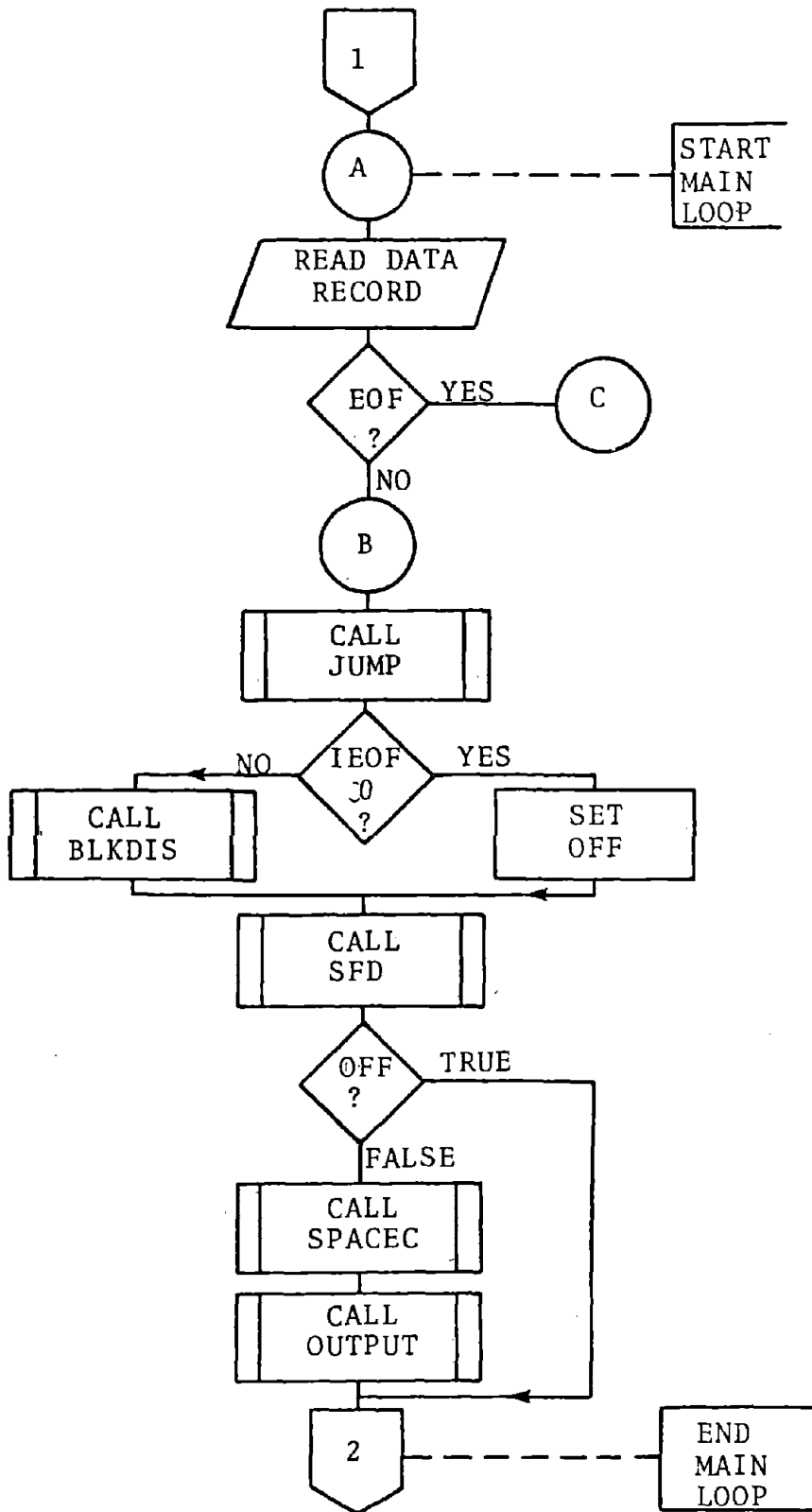


Figure 15 (continued).

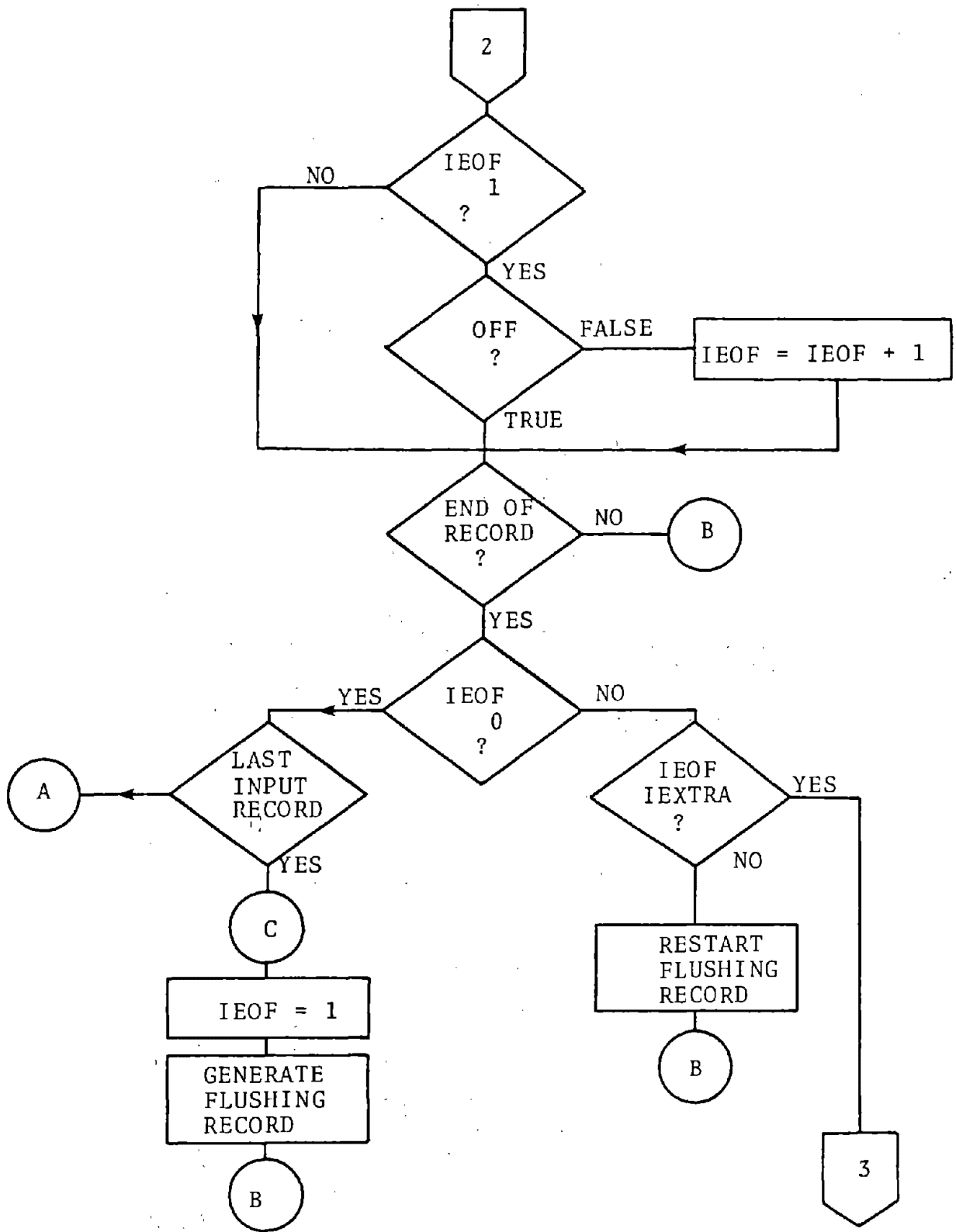


Figure 15 (continued).

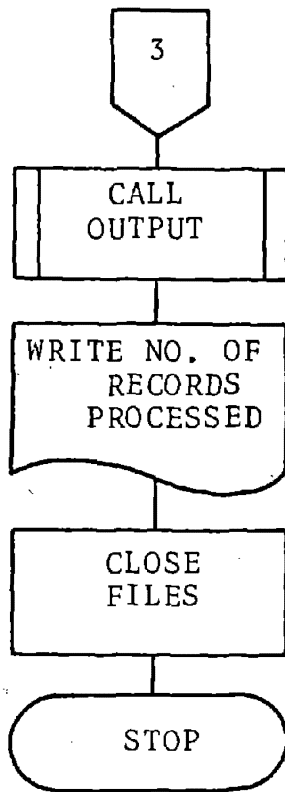


Figure 15 (concluded).

unit 9. The specific form of the input is covered in Part 1, Section 2.5.2, of this report.

6.3 OUTPUT DATA

Similarly, the output is in two forms, the run parameters and other information documenting the run, which are written to unit 6, and the processed data, which are written to unit 10. The specific form of the output is described in Part 1, Section 2.5.3, of this report.

6.4 PROGRAM CONSTANTS

The program contains constants initialized through DATA statements. A few of these constants may have to be changed if operating conditions change. The specific constants involved and instructions for changing them are covered in Part 2, Section 5, of this report.

6.5 SOURCE CODE

The FORTRAN source code listings for the main program and the five subroutines are provided in Appendix B.

6.6 COMMON BLOCKS

There are five common blocks in the program. These are described in Appendix C.

7.0 RESULTS

When the profilometer data were being collected for this project, the acoustic probe was experiencing some signal dropout problems that greatly reduced its data-gathering ability. Consequently, it was not possible to collect any road profile data, but a limited amount of data were obtained indoors using simulated pavement motion. The data collected and the results obtained from it are described below.

There are plans to collect road profile data and thus demonstrate the data processing system more completely when the acoustic probe is performing better.

7.1 EQUIPMENT SETUP

A horizontal board approximately twenty inches (51 cm) square and 1/4 inch (6 mm) thick was attached to an oscillating drive mechanism so that it moved vertically (perpendicular to the plane of the board). The amplitude of the motion was 3/16 inch (4.8 mm) zero-to-peak. The usable speeds ranged from 0.5 Hz, where it was limited by chatter and lack of power to lift the board, to 5 Hz, which approached the board's resonance frequency.

The board was placed under the acoustic probe, and the vehicle was raised so that the probe-to-board distance was the same as the normal probe-to-pavement distance.

The accelerometer was removed from its normal location on the acoustic probe and attached to the board without changing its orientation. With this arrangement, the acoustic probe and the accelerometer measure the same motion, and their effects are additive in the digital processing. This situation contrasts with the normal one where the accelerometer is on the acoustic probe and the vehicle is bounced over a stationary

surface, in which case the two measurements tend to cancel each other (see Part 2, Section 4, of this report). However, mathematically it is only a change of the sign on one of the signals to obtain an effect of cancellation, which is useful in calibrating the system.

The block distance signal was generated by feeding a periodic pulse into the ENSCO Electronic Package (EEP) at a rate sufficient to produce 500 block distance pulses per second (see Part 2, Section 3.2).

With the above exceptions, the equipment was set up according to Part 1, Section 2.1, of this report.

7.2 DATA AVAILABLE

Data are available for six runs made with the oscillating board. Ten feet (3 m) of analog tape were recorded per run, which provides sixteen seconds of data per run. For the first three runs, the standoff (probe-to-board) distance was adjusted so that there were no phase jumps in the acoustic probe signal. For the last three runs, the standoff distance was changed to give a pair of phase jumps per cycle of oscillation.

The six runs are listed in Table 4. The pavement wavelength values correspond to the assumption of a one-inch (2.5 cm) block distance interval. Runs 1 and 6 are considered long wavelength runs, runs 2 and 5 are medium wavelength, and runs 3 and 4 are short wavelength. (Although the data processing system is capable of handling a wider range of wavelengths than this, the oscillating board is incapable of generating them.)

The mean standoff height (to the bottom surface of the acoustic probe) was 8.5 inches (21.6 cm) for runs 1-3, 7.75 inches (19.7 cm) for run 4 and 7.62 inches (19.4 cm) for runs 5-6.

TABLE 4

Characteristics of the Six Runs

Run	Phase Jumps	Frequency (Hz)	Wavelength (feet)	Wavelength (meters)
1	no	0.507	82.5	25.1
2	no	2.84	14.7	4.49
3	no	5.15	8.13	2.48
4	yes	5.24	8.01	2.44
5	yes	2.96	14.2	4.31
6	yes	0.739	56.7	17.3

7.3 PHASE JUMP RESULTS

No phase jumps exist in the data for runs 1-3, and the phase jump processing does not erroneously detect any jumps for these runs.

Runs 4-6 are more interesting in this regard because phase jumps are inserted deliberately. Figure 16 shows the raw phase angle input and the reconstructed phase angle signal after phase jump processing for runs 4-6. The results for runs 4 and 5 are perfect, but there are two slight flaws, indicated by (1) and (2), in run 6.

The flaws in run 6 occur because the jump occurs in this run at a point where the phase angle changes especially slowly with time, and consequently the phase meter introduces extraneous jumps as it hovers near the switching point. Figure 17a shows the time-based input to phase jump processing in the vicinity of the pair of jumps (1) in Figure 16c. Just after the jump up, there is a notch corresponding to a pair of extraneous jumps spaced so closely that the signal does not have time to reach the zero degree level. Consequently, no phase jump is detected at the notch, and the notch passes through to the output.

Figure 17b corresponds to the pair of jumps indicated at (2) in Figure 16c. In this case there is an extraneous spike just before the jump up. Because the spike has too little duration to reach full 360 degree height, it too is undetected and thus appears in the output.

The next pair of jumps, indicated (3) in Figure 16c, have no flaws in the output, but there is indication of a flaw at the jump up in the input. Figure 17c shows the flaw in the enlarged time-based format. In this case there is enough time for the signal to jump from 0 to 360 degrees or vice versa, and three jumps - up, down, up - are detected and corrected.

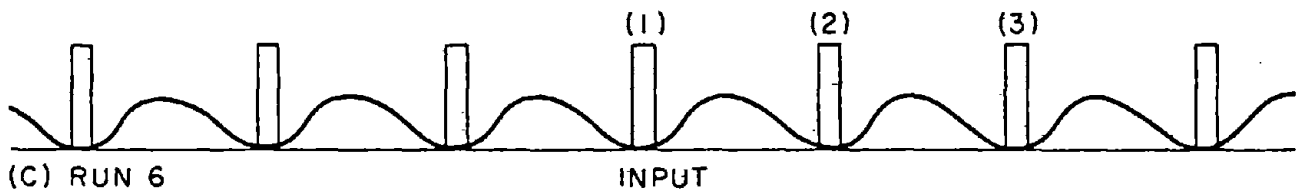
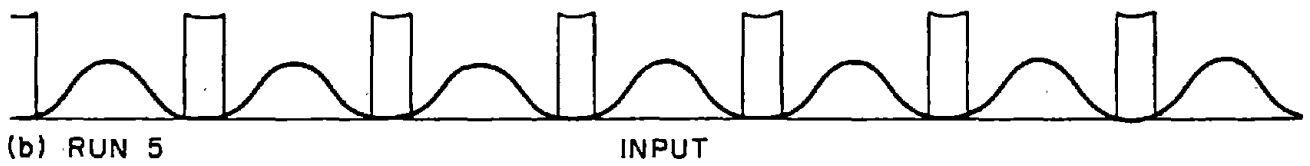
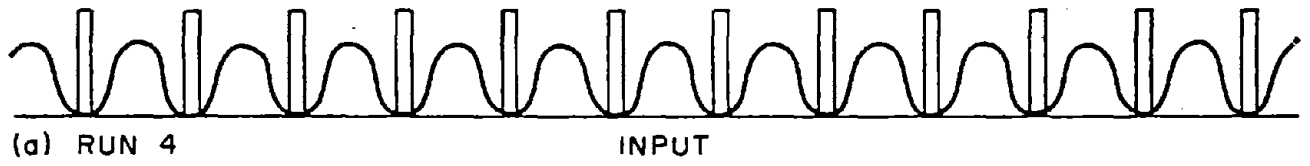
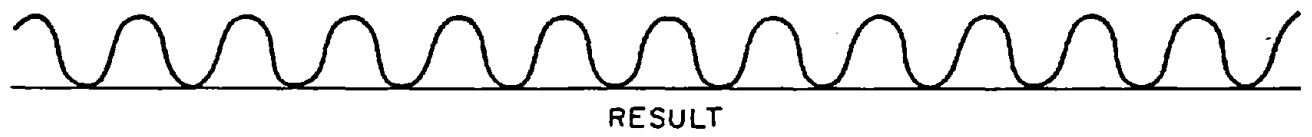
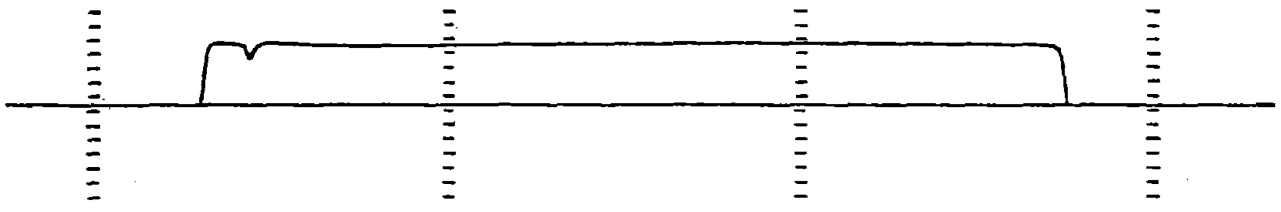
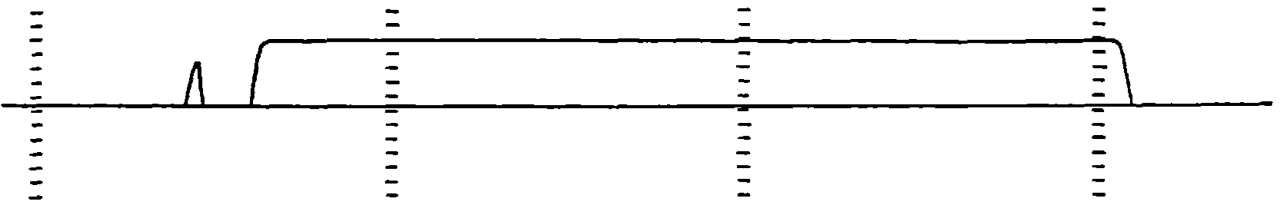


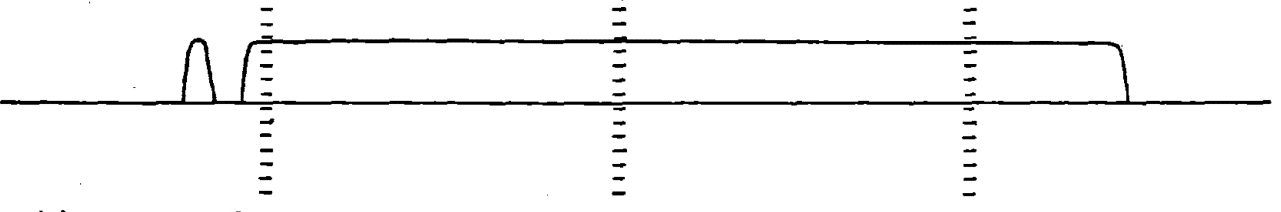
Figure 16. Phase Jump Processing for Runs 4-6.



(a) REGION 1



(b) REGION 2



(c) REGION 3

Figure 17. Time-Based Enlargements of Three Regions in Figure 16c.

Besides (3), there are two other cases of this type evident in Figure 16c, and all three are handled properly by the phase jump processing.

The digital phase jump processing produces a much smoother result than the range extender it replaces. Figure 18 illustrates the range extender's performance on periodic signals similar to those in Figure 16. Note that there is a significant spike in the output each time a phase jump occurs.

7.4 PROFILE AMPLITUDE RESULTS

The oscillating board has an amplitude of 3/16 inch (4.8 mm), and because of the way the equipment was set up, the computed profile would be expected to have an amplitude of twice this amount, or 3/8 inch (9.5 mm). The results actually computed for profile amplitude are given below.

Because of difficulties encountered with the acoustic probe, it was not possible to obtain an accurate vertical calibration of the system, but an approximate calibration was obtained by calculating the overall system gain from individual component gains. Table 5 shows the amplitudes computed for the six runs relative to the amplitude of the oscillating board.

The results expected for phase jump processing output are 1.000 for all runs. The actual results fall considerably short of this value, probably because of inaccurate vertical calibration and nonlinear acoustic probe response¹⁵. Observe that the phase jump processing output is particularly small for runs 1-3. Data for these runs were collected with an 8.5 inch (21.6 cm) stand-off height, and it is known that the sensitivity of the acoustic probe is particularly low at this height.

¹⁵ Ideally, the probe's output phase angle is proportional to the input probe-to-pavement displacement. Stray acoustic paths inside the probe, however, cause the actual response to deviate substantially from ideal linear performance.

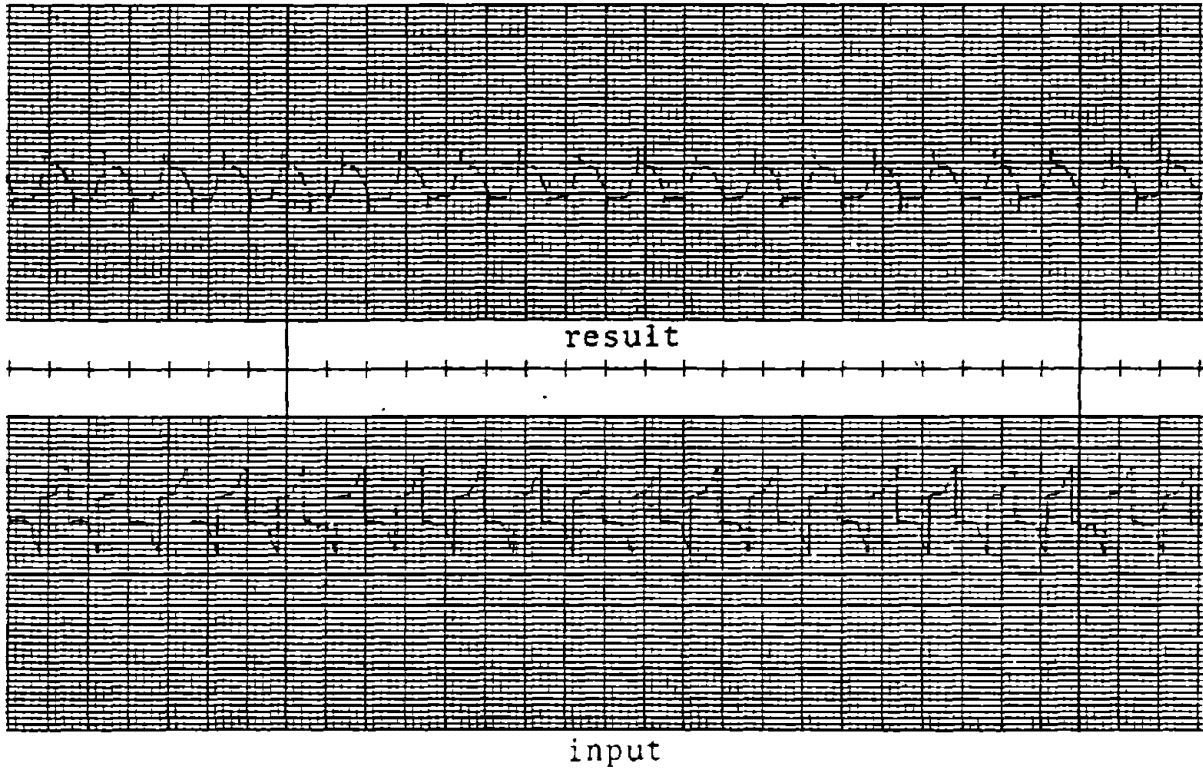


Figure 18. Range Extender Performance

TABLE 5

Profile Amplitude Results
(Displacement Relative to Input Displacement)

Run	Phase Jump Processing Output	Space Curve Processing Output	Apparent Accelerometer Component
1	0.232	1.197	0.965
2	0.248	1.237	0.989
3	0.384	1.379	0.995
4	0.939	1.947	1.008
5	0.773	1.763	0.989
6	0.693	1.667	0.973

Another observation can be made from the phase jump processing output in Table 5. The high frequency runs (runs 3 and 4; see Table 4) have large amplitudes relative to the low frequency runs (runs 1 and 6). This occurs because the high frequency runs are close to resonance of the oscillating board, which is a condition in which the part of the board under the acoustic probe is flapping with greater amplitude than the driven motion at the root of the board.

The space curve processing output listed in Table 5 follows the same pattern among runs as discussed above for the phase jump processing output. By subtracting these two amplitudes for each run, the displacement amplitude apparently due to the accelerometer measurement can be calculated. These values are listed in the last column in Table 5, and they all fall close to the expected value of 1.000. The high frequency runs have somewhat greater amplitude, which occurs because the accelerometer is mounted slightly outboard of the root of the board.

The fact that the values in the last column of Table 5 are approximately the same for all six runs means that the processing is correct under this variety of conditions. The fact that all six values are approximately 1.000 means that the approximate calibration for the accelerometer is correct within three percent. The fact that there is substantial variation among the six phase jump processing outputs only indicates that the acoustic probe is nonlinear and out of calibration and that the oscillating board was operated too close to its resonance; this variation does not detract from the correctness of the data processing system.

7.5 SIGNAL CANCELLATION RESULTS

The vertical acceleration calibration procedure calls for rocking the vehicle over fixed pavement and adjusting the scale factor ratio until the accelerometer and noncontact sensor

channels just cancel each other (see Part 2, Section 4). With the oscillating board, a similar situation can be created by using negative values of scale factor ratio to invert the accelerometer signal. Results obtained in this way are discussed below.

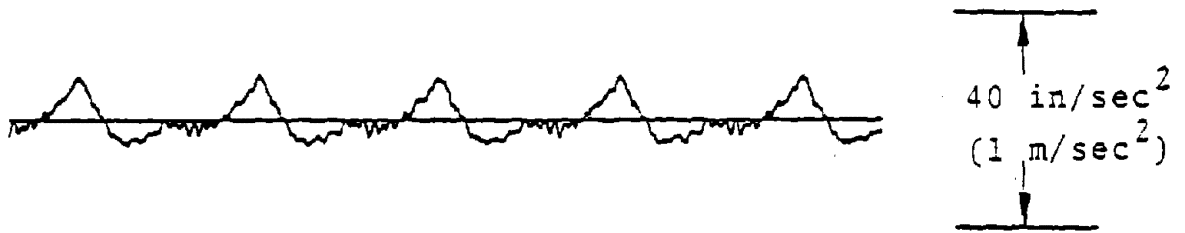
The six runs listed in Table 5 are obtained using a scale factor ratio of $446/\text{sec}^2$. With a scale factor ratio of $-446/\text{sec}^2$, partial cancellation is obtained in all six cases. Cancellation is partial in the three cases corresponding to runs 1-3 because the acoustic probe sensitivity is low for these three runs, as discussed in Section 7.4. In the two cases corresponding to runs 4 and 5, the acoustic probe sensitivity is improved, but there is a phase shift in the oscillating board because it is operating close to resonance. The board's phase shift introduces a phase shift into the processing so that complete cancellation is not possible.

This leaves the case corresponding to run 6 as the best opportunity to demonstrate cancellation. Figures 19a-19c show the noncontact sensor signal, the accelerometer signal and the output profile, respectively, for run 6. When the accelerometer signal is inverted, Figure 19d results, and it is clear that the two input signals cancel each other to a great extent. Further examination reveals that the accelerometer signal is overcancelling the noncontact sensor signal, so in Figure 19e the accelerometer gain is reduced to $3/4$ of its previous value. The result is good cancellation. (Observe that Table 5 would suggest that a scale factor ratio of $-446(0.693/0.973)\text{sec}^{-2} = -318/\text{sec}^2$ be used to obtain cancellation with the run 6 data.)

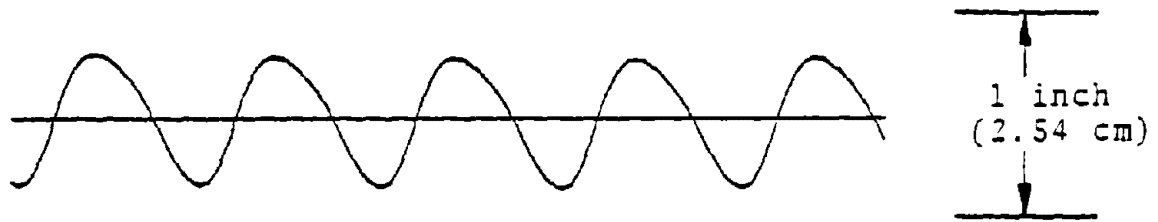
7.6 SPACE CURVE FILTERING RESULTS



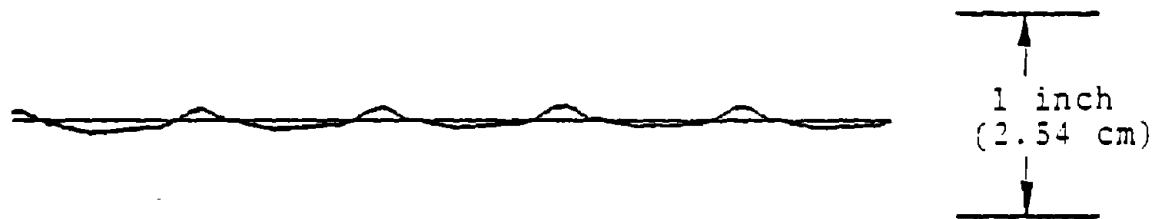
a) Noncontact sensor signal



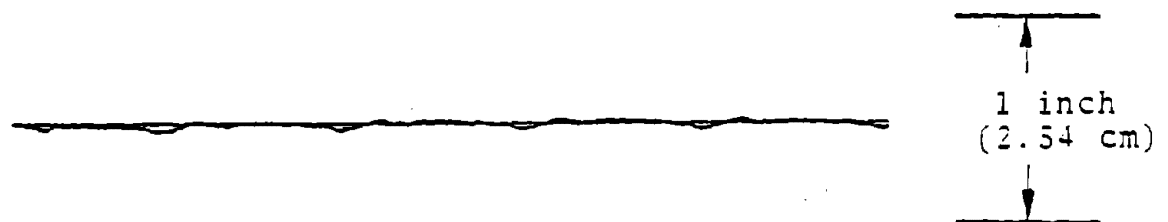
b) Accelerometer signal



c) Output profile (SCALE = 446/sec²)



d) Output profile (SCALE = 446/sec²)



e) Output profile (SCALE = 334/sec²)

Figure 19. Signal Cancellation Results

7.6.1 FILTER CUTOFF CHARACTERISTICS

The space curve filter's theoretical frequency response is shown in Figure 14 [Z(ϕ)], and the corresponding cutoff wavelengths are given in Table 2. The actual frequency response is determined here by processing the data from runs 1-6 with various combinations of filter parameters chosen to place the fundamental frequency of the oscillating board in the cutoff region.

Two parameters influence the cutoff wavelength: the space curve filter exponent, n , and the distance sample interval, D . The cutoff ($1/\sqrt{2}$ amplitude) wavelength, λ_c , is

$$\lambda_c = 1.843 D (2^n - 1). \quad (105)$$

All of the data collected for runs 1-6 correspond to $D = 1$ inch (2.5 cm). In order to obtain data with larger values of D for this exercise, however, the collected data have been processed to remove selected block distance pulses so as to create data with larger values of D .

Table 6 presents results for fourteen runs. Runs 1-6 are the ones that have been discussed up to this point. The values of n and D used for these runs are shown in the table. The corresponding value of ψ [$\psi = (2^n - 1) \phi D$, where ϕ , the spatial frequency, is the reciprocal of the listed wavelength] is greater than unity for runs 1-6. Therefore, all six of these runs lie in the range of spatial frequencies passed by the space curve filter (see Figure 14).

Runs A-H use the same noncontact sensor and accelerometer data as runs 1-6¹⁶, but the values of n and D are changed so that all eight of these runs lie in the range $0 < \psi < 1$ where the

¹⁶Runs A-H are based on runs 1, 2, 3 and 6 as indicated in Table 6. Run 4 is not used as a basis because it has essentially the same wavelength as run 3, and likewise for run 5.

TABLE 6
Space Curve Filter Cutoff Results
(1 foot = 12 inches = 30.5 cm)

Run	Wavelength (feet)	n	D (inches)	ψ	$Z^A(\psi)$	Runs Compared	Theoretical Amplitude Ratio	Measured Amplitude Ratio
1	82.5	8	4	1.0303	1.0000	--	--	--
2	14.72	8	1	1.4436	1.0152	--	--	--
3	8.131	7	1	1.3016	1.0104	--	--	--
4	8.014	7	1	1.3206	1.0115	--	--	--
5	14.14	8	1	1.5028	1.0143	--	--	--
6	56.7	8	4	1.4991	1.0144	--	--	--
A(1)	82.5	8	1	0.2576	0.0972	A:1	0.0972	0.1823
B(1)	82.5	8	2	0.5152	0.6477	B:1	0.6477	0.6494
C(2)	14.72	5	1	0.1755	0.0247	C:2	0.0243	0.0555
D(2)	14.72	6	1	0.3567	0.2710	D:2	0.2669	0.2912
E(3)	8.131	5	1	0.3177	0.1919	E:3	0.1899	0.2082
F(3)	8.131	6	1	0.6457	0.8787	F:3	0.8697	0.8759
G(6)	56.7	7	1	0.1867	0.0310	G:6	0.0306	0.0898
H(6)	56.7	8	1	0.3748	0.3114	H:6	0.3070	0.3768

signal is attenuated according to Figure 14. Quantity

$$Z^*(\psi) = Z(\phi) = Z\{\psi/[(2^n-1)D]\}$$

is the theoretical fraction of the signal passed by the filter.

Table 6 shows the basis run (runs 1-6) against which each of the runs A-H is compared. The theoretical amplitude ratio is obtained by dividing values of Z^* for the two runs involved. The measured amplitude ratio - the last column in Table 6 - is obtained by dividing amplitudes of the output profiles for the two runs.

The theoretical and measured amplitude ratios compare well in all eight cases, which demonstrates the correctness of the space curve filtering cutoff.

In all eight cases the measured amplitude ratio is larger than the theoretical ratio. This occurs because the oscillating board produces harmonics that are above the spatial cutoff frequency, and these harmonics are passed by the filter without attenuation, thus inflating the measured amplitude ratio. The long wavelength runs (runs A, B, G and H) have the largest discrepancy between theoretical and measured amplitude ratios because these runs have the largest amount of higher harmonics. (In these low frequency runs the oscillating board's drive motor is taxed. Consequently, the board rises more slowly than it falls, and the board also tends to chatter, as indicated in Figure 19b.)

7.6.2 FILTER PARAMETER TRADEOFFS

Table 2 indicates that several combinations of n and D often yield similar cutoff wavelengths. The question arises: when alternative values of n and D will produce the desired cutoff wavelength, how should n and D be chosen? This section discusses the tradeoffs involved.

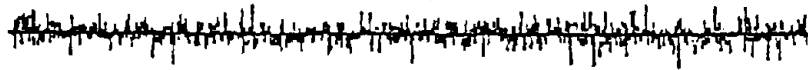
As an example, consider run 2. Table 6 shows that up to this point, this data has been processed with $n = 8$, $D = 1$ inch (2.5 cm). But Table 2 indicates that a similar cutoff wavelength [39 feet (12 m)] can also be obtained with $n = 7$, $D = 2$ inches (5 cm); $n = 6$, $D = 4$ inches (10 cm); and $n = 5$, $D = 8$ inches (20 cm). Table 7 lists the four alternatives for the run 2 data.

TABLE 7
Space Curve Filter Alternatives

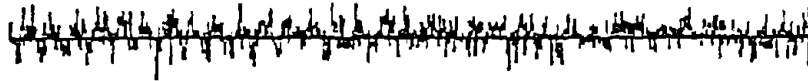
n	D (inches)	D (cm)	Relative Computer Time
8	1	2.5	1.000
7	2	5	0.985
6	4	10	0.950
5	8	20	0.820

This table illustrates that alternatives with large D take less computer time because the distance-based calculations are done less frequently. It is also clear that the time-based calculations must consume most of the computer time because not too much time can be saved by using a larger value of D .

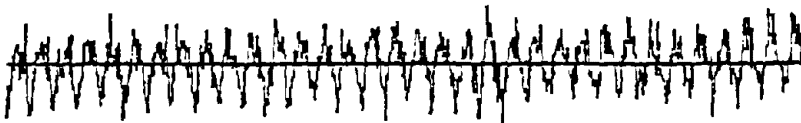
Figure 20 illustrates a more pertinent aspect of the alternatives, namely, the SFDs generated in the four cases. The wavelengths of interest are much longer than D , and in this case the SFD associated with the wavelength of interest is proportional to D^2 . The SFD associated with noise in the measurements or computations, however, is independent of D . Therefore, the signal-to-noise ratio is low for small values of D .



a) $n = 8$, $D = 1$ inch (2.5 cm)



b) $n = 7$, $D = 2$ inches (5 cm)



c) $n = 6$, $D = 4$ inches (10 cm)



d) $n = 5$, $D = 8$ inches (20 cm)

Figure 20. SFD Traces for Alternative Filters Having the Same Cutoff Wavelength (All are Plotted to the Same Scale)

This problem is compounded by the fact that an alternative with a small D has a large n , and the space curve processing requires a larger dynamic range when n is large.

All four alternatives have the same cutoff wavelength and produce the same profile when the wavelengths of interest are much larger than D . Because the alternative with a large value of D is superior computationally, it is preferred unless it is desired to recover very short wavelengths.

8.0 SUMMARY AND CONCLUSIONS

A hybrid data processing system has been developed for inertial based road profilometers; the output is distance-based and accurately recovers profile wavelengths up to 300 feet (90 m). The inertial base is established by an accelerometer vertically mounted on a survey vehicle; the distance from the inertial accelerometer to the road surface could be a displacement transducer or a velocity transducer, either contact or noncontact type. The present system uses a noncontact acoustic system which measures displacement.

With the present system, analog processing is done online. Processed transducer signals and a block distance signal generated by a wheel-driven tachometer are recorded on analog magnetic tape. The analog tape is then taken to a computer facility where the analog data is converted to digital form at a scan rate of 4000Hz, which is then processed by off-line computer programs to produce a distance-based, speed invariant profile measurement.

Digitizing and digital processing are done off-line. The need to perform off-line digitizing and processing means a long delay between taking a measurement and seeing the result. It would be much more desirable to perform all necessary processing onboard which will eliminate the need for intermediate analog recording and provide profile measurement results while conducting the survey. This is, in fact, the goal of the development effort.

As a part of this project, ENSCO completed the preliminary design of an online system using a Texas Instruments Model 990/10 minicomputer. The off-line software developed under this project employed the concept of an online system; i.e., it receives data streams scan-by-scan as they are provided by

a real-time analog-to-digital converter, and performs the necessary delays and recursive processing to provide a continuous profile output. Adaptation of this software into an online, near real-time system is relatively easy. This off-line software also has the built-in capability to accept acceleration, velocity and displacement measurements so that different types of transducers can be used in the system.

9.0 RECOMMENDATIONS

Testing of the hybrid processing system has been hampered by the inability to collect reliable road data with the acoustic probe. When the acoustic probe is working properly, it would be advisable to collect and process some road profile data to further verify the data processing capabilities. Specifically, it would be desirable to demonstrate that profile wavelengths as short as six inches (0.2 m) can be recovered and that the system is speed and direction invariant.

Now that the feasibility of recovering road profiles accurately with hybrid processing has been demonstrated, FHWA should proceed to develop an online system employing the same techniques. The online system provides an accurate profile measurement on the spot, which is a quality needed to make this system attractive to the highway community.

The present offline system has been developed under the assumption that it would be converted to an online system soon. If, on the contrary, the offline system is the end product, then some small changes would make it more useful. One is a digital preprocessing capability to eliminate block distance pulses as desired so that various distance sample intervals can be used at the digital processing stage (see Section 7.6). This capability could also expand the repertoire of filter cutoff wavelengths.

Another suggested addition to the offline processing is a post-processing capability. Right now the profile results are just written on a magnetic tape. In order to use these results, it is necessary to list them on a printer, plot them, or perform further calculations, such as computing power spectral density.

Had road profiles been collected during this project, the question that would have arisen is whether the computed profiles are correct. In order to answer such questions, a means is needed for constructing or measuring a calibrated surface so that the accuracy of profilometers can be determined. It is recommended that FHWA obtain a known highway profile for testing road profilometers.

APPENDIX A
CALCULATION OF THE ACCELERATION BIAS

The acceleration bias is obtained from the average accelerometer reading over the first n_{\max} time-based samples of the run. For time step $n_2 \leq n_{\max}$, the average is

$$b_{n_2} = \frac{1}{n_2} \sum_{i=1}^{n_2} a_i \quad (\text{A-1})$$

Observe that

$$a_{n_2} = \sum_{i=1}^{n_2} a_i - \sum_{i=1}^{n_2-1} a_i \quad (\text{A-2})$$

which by use of Equation (A-1) becomes

$$a_{n_2} = n_2 b_{n_2} - (n_2 - 1) b_{n_2-1} \quad (\text{A-3})$$

Rearrangement yields

$$b_{n_2} = b_{n_2-1} - (b_{n_2-1} - a_{n_2})/n_2 \quad (\text{A-4})$$

In computational notation this equation is

$$b \leftarrow b - (b - a)/n_2 \quad (\text{A-5})$$

Equation (A-5) is used for $1 \leq n_2 \leq n_{\max}$. For $n_2 > n_{\max}$ the existing value of b is used without further updating of b .

APPENDIX B
COMPUTER PROGRAM SOURCE LISTINGS

```

C      ROUTINE TO PROCESS FHWA NONCONTACT HIGHWAY PROFILEMETER DATA
C      FHWA CONTRACT NO. DOT-FH-11-9551
C      ENSCO, INC., SPRINGFIELD, VIRGINIA
C      WRITTEN AUGUST 21, 1979 BY G. D. GUNN AND J. C. CORBIN
C      MODIFIED DECEMBER 26, 1979 BY P. G. SMITH
C
COMMON /IN/ IRAW(3,256)
COMMON /OUT/ IPROC(7,256)
COMMON /WORK/ IDOUT(7)
COMMON /PAR/ FREQ,RHO1,RHO2,OMEGA2,OMT2,SCALE
COMMON /HW/ NU(4),C1,C2
LOGICAL OFF,CLOS
INTEGER TAPE0,TAPE1,TAPE2
DIMENSION TITLE(20),ALPHA(8)
DATA ALPHA/'DISP','LACE','MENT','VELO','CITY','
' 'X2 ',' ' //
DATA TAPE0,TAPE1,TAPE2 /9,9,10/,
*IEOF,NSTEP,NSTEP,CLOS,MOUT/0,1,0,.FALSE.,0/

C
C      TAPE0 IS UNIT TO READ TAPE TITLE: =9, TITLE ON RAW TAPE
C      OTHERWISE, =5, =>READ TITLE CARD
C      TAPE1 (=9) IS THE INPUT RAW DATA TAPE (TIME BASED)
C      TAPE2 (=10) IS THE OUTPUT PROCESSED DATA TAPE (DISTANCE BASED)
C
REWIND TAPE1
REWIND TAPE2
IDOUT(6)=0
IDOUT(7)=0

C
C READ THE RUN PARAMETERS
C
IF(TAPE0.EQ.9)READ(TAPE0)TITLE
IF(TAPE0.EQ.5)READ(5,10)TITLE
10 FORMAT(20A4)
READ(3,3) MIN,MAX
3 FORMAT(2I10)
READ(3,4) FREQ,NFIL,MODE,SCALE,OMEGAA,OMEGA V
4 FORMAT(F10.0,2I10,3F10.0)

C
C SET UP PROCESSING CONSTANTS
C
IF(MODE) 7,7,8
7 RHO1=1.
RHO2=0.
MODE=0
GO TO 9
8 RHO1=1./OMEGA V
RHO2=OMEGAA
MODE=1
9 OMA2=OMEGAA**2
OMT2=0.5*OMEGAA/FREQ
IF(NFIL.LT.5) NFIL=5
IF(NFIL.GT.8) NFIL=8
C2=2.**NFIL-1.
C1=-(C2**2-1.)/8.
NU(1)=1
NU(2)=(C2+1)/2
NU(3)=C2
NU(4)=C2+1
IEXTRA=5*(C2-1)/2+2

C
C      TITLE IA A HEADER IDENTIFYING THE RUN DATA
C      MIN IS THE FIRST RECORD TO PROCESS
C      MAX IS THE LAST RECORD TO PROCESS

```



```

C      FREQ IS THE DIGITIZATION FREQUENCY
C      NFIL IS THE SPACE CURVE FILTER CUTOFF EXPONENT (USE 5,6,7 OR 8)
C      MODE IS THE SENSOR MODE FLAG: 0 FOR DISPLACEMENT, 1 FOR VELOCITY
C      SCALE IS THE RATIO OF SCALE FACTORS FOR ACCELERATION TO
C      NONCONTACT SENSOR
C      OMEGA0 IS THE ACCELERATION FILTER CORNER FREQUENCY
C      OMEGA1 IS THE VELOCITY FILTER CORNER FREQUENCY
C
C      WRITE(TAPE2) TITLE
C
C      SKIP TO PROPER PLACE ON THE TAPE
C
C      IF(MIN.LE.1)GO TO 50
      NSKIP=MIN-1
      DO 40 I=1,NSKIP
      READ(TAPE1,END=2000) IRAW
40     CONTINUE
C
50     CONTINUE
      IF(MAX.LE.MIN)MAX=32000
      NREC=MAX-MIN+1
      I1=MODE*3+1
      I2=I1+2
      I3=MODE+7
      WRITE(6,20) TITLE,MIN,MAX,NREC,FREQ,NFIL,(ALPHA(I),I=I1,I2),
      ISCALE,ALPHA(I3),OMEGA0,OMEGA1
20     FORMAT(///5X,20A4//5X,'READ FROM ',I3,' TO ',I5,' : ',
      I5,' RECORDS'//5X,'DIGITIZATION FREQUENCY = ',F8.1,
      ' SCANS/SEC'//5X,'FILTER EXPONENT = ',I2//5X,'SENSOR MODE: ',
      I3A4//5X,'SCALE FACTOR RATIO = ',1PE12.4,' /SEC',A4//5X,'ACCELEH',
      'ATION CUTOFF FREQUENCY = ',1PE12.4,' RAD/SEC'//5X,'VELOCITY ',
      'CUTOFF FREQUENCY = ',1PE12.4,' RAD/SEC'//1X,80(' '))
C
C      MAIN PROCESSING LOOP
C
      DO 700 NR=1,NREC
      READ(TAPE1,END=900) IRAW
      ISAVE=IRAW(2,254)
150     CONTINUE
      DO 500 I=1,254
      IDOUT(1)=IRAW(2,I)
CHECK  FOR PHASE METER JUMP
      CALL JUMP(I,ISLK,IPRS,IACCEL)
      IDOUT(2)=IPRS
      IDOUT(3)=IACCEL
      NSTEP=NSTEP+1
      IF(IEOF) 60,60,70
CHECK  FOR BLOCK DISTANCE INTERRUPT) SET OFF TO FALSE IF SU
60     CALL BLKDIS(ISLK,OFF)
      IF(OFF) GO TO 80
      NSTEP=NSTEP
      NSTEP=0
      GO TO 80
C
C      IF FLUSHING AT THE END OF A RUN (IEOF.GT.0), SET THE VALUE OF 'OFF'
C      WITHOUT USING BLOCK DISTANCE PULSES
C
70     OFF=.TRUE.
      IF(NSTEP.LT.NSTEP) GO TO 80
      OFF=.FALSE.
      NSTEP=0
CONVERT TIME-BASED DATA INTO DISTANCE-BASED SECOND FINITE DIFFERENCES
80     CALL SFD(IPRS,IACCEL,OFF,DELTA)
CONVERT SECOND FINITE DIFFERENCES INTO SPACE CURVES
      IF(OFF)GO TO 400
      CALL SPACEC(DELTA,SPCV)

```

```

C SEND OUTPUT TO TAPE
  IDOUT(4)=DELTA
  IDOUT(5)=SPCV
  CALL OUTPUT(TAPE2,CLOS,MOUT)
400 IF(IEOF.GE.1.AND..NOT.NOF) IEOF=(IEOF+1)
500   CONTINUE
C
C AFTER PROCESSING THE GIVEN DATA, PROCESS MORE RECORDS OF BLANK DATA
C TO GET THE SPACE CURVE OUTPUT FOR THE LAST INPUT DATA
C
  IF(IEOF.LE.0)GO TO 700
  IF(IEOF.GT.IEXTRA)GO TO 1000
  GO TO 150
700   CONTINUE
C
C GENERATE BLANK DATA
C
900   CONTINUE
  IEOF=1
  IF(MODE.GT.0) ISAVE=0
  DO 950 I=1,254
  IRAW(2,I)=ISAVE
  IRAW(3,I)=0
950   CONTINUE
  GO TO 150
C
C CLOSE OUT RUN
C
1000  CONTINUE
  CLOS=.TRUE.
  CALL OUTPUT(TAPE2,CLOS,MOUT)
  NR=NR-1
  WRITE(6,1010) NR,MOUT
1010  FORMAT(5X,I3,' INPUT RECORDS PROCESSED'//
  5X,I3,' OUTPUT RECORDS GENERATED'////)
  REWIND TAPE1
  ENDFILE TAPE2
  REWIND TAPE2
  STOP
2000  CONTINUE
  WRITE(6,2050) 1
2050  FORMAT(///5X,'SKIP ERROR, EOF AT ',I3///)
  STOP
  END

```

```

SUBROUTINE SFD(IPRB,IACCEL,OFF,DELTA)
C
C PREPARES ACCELEROMETER AND NONCONTACT SENSOR SIGNALS, AND COMBINES
C THEM TO GIVE A SECOND FINITE DIFFERENCE OF PAVEMENT PROFILE
C
LOGICAL OFF,FLAG
COMMON /PAR/ FREQ,RHO1,RHO2,QMA2,OMT2,SCALE
DATA N1,N2,IBIAS/0,1,10000/
DATA ASO,BIAS,AAO,DAO,FA,GA,HA,AA1,AA1,CC1,GA1,HA1,FA1/1JXO./
C
C TIME-BASED SECOND FINITE DIFFERENCE (INNER LOOP)
C
AS=FLOAT(IPRB)
US=AS+ASO
ASO=AS
AA=FLOAT(IACCEL)*SCALE
IF(N2.GT.IBIAS)GO TO 10
BIAS=BIAS-(BIAS-AA)/FLOAT(N2)
N2=N2+1
10 CONTINUE
CA=AA+AAO+RHO2*US
DA=AA+AAO-2.*BIAS
EA=DA+DAO
AAO=AA
DAO=DA
C
FA=FA+CA
GA=GA+EA
HA=HA+GA
N1=N1+1
IF(OFF)RETURN
C
C DISTANCE-BASED SECOND FINITE DIFFERENCE (OUTER LOOP)
C
US=AS-AS1
CC=AA-AA1+RHO1*QMA2*US
DELTA=CC-CC1+(FA-FA1)*OMT2+(HA+FLOAT(N1)*GA1-HA1)*OMT2*OMT2
DELTA=DELTA/QMA2
C
AA1=AA
CC1=CC
GA1=GA
FA1=FA
HA1=HA
AS1=AS
C
FA=0.
GA=0.
HA=0.
N1=0
RETURN
END

```

```

SUBROUTINE BLADIS(IBLK,OFF)
C
C DETECTS APPEARANCE OF BLOCK DISTANCE PEDISTAL
C USING FIRST DIFFERENCE OF THE SIGNAL
C
LOGICAL OFF,FLIP
COMMON /PAR/ FREQ,RHO1,RHO2,OMA2,OMT2,SCALE
DATA FLIP /.FALSE./, THRESH/400./
C
C FLIP IS FALSE UNTIL NEGATIVE THRESHOLD; RESET TO FALSE
C AT POSITIVE THRESHOLD
C
OFF=.TRUE.
R1=FLOAT(IBLK)
TEST=R1-R0
R0=R1
IF(ABS(TEST).GE.THRESH)GO TO 100
50 CONTINUE
RETURN
C
100 CONTINUE
IF(ABS(TEST).LT.0)GO TO 110
110 CONTINUE
FLIP=.FALSE.
GO TO 50
120 CONTINUE
IF(FLIP)RETURN
FLIP=.TRUE.
OFF=.FALSE.
RETURN
END

```



```

SUBROUTINE OUTPUT(ITAPE,CLOS,MOUT)
C
C WRITES 7X256 RECORD TO TAPE
C
      LOGICAL CLOS
      COMMON /OUT/ (PROC(7,256)
      COMMON /WORK/ IDUM(7)
      DATA MOUT/1/
C
C OUTPUT CHANNEL ASSIGNMENTS
C 1: RAW NONCONTACT SENSOR SIGNAL
C 2: NONCONTACT SENSOR PROCESSED TO REMOVE JUMPS
C 3: RAW ACCELEROMETER SIGNAL
C 4: SECOND FINITE DIFFERENCE
C 5: SPACE CURVE
C
      IF(CLOS) GO TO 30
      DO 10 I=1,7
      IPROC(I,MOUT)=(DOUT(I)
10      CONTINUE
      IF(MOUT.LT.256)GO TO 20
      WRITE(ITAPE) IPROC
      MOUT=MOUT+1
      MOUT=0
20      CONTINUE
      MOUT=MOUT+1
      RETURN
C
C CLOSE OUT LAST OUTPUT RECORD
C
30 IF(MOUT.LE.1) RETURN
      DO 40 J=MOUT,256
      DO 40 I=1,7
40 IPROC(I,J)=0
      WRITE(ITAPE) IPROC
      MOUT=MOUT+1
      RETURN
      END

```

```

SUBROUTINE SPACED(Delta,SPCV)
C
C GENERATES SPACE CURVE FROM SECOND FINITE DIFFERENCE
C
DOUBLE PRECISION XL0,XL1,XX(7)
DIMENSION AUG(5,256),SPCURV(3,256)
COMMON /HW/ NU(4),C1,C2
DATA AUG,SPCURV,XL0,XL1,XX/2048*0.,9*0.DO/
C
C CALCULATE BIAS TERM
C
BIAS=DELTA
DO 10 I=1,5
AUG(I,NU(1))=BIAS
XX(I)=XX(I)+BIAS-AUG(I,NU(4))
BIAS=XX(I)/C2
10 CONTINUE
C
C FIRST SPACE CURVE
C
XL0=XL0+AUG(1,NU(2))-XX(1)/C2
XL1=XL1+XL0
C
C HIGHER ORDER SPACE CURVE
C
SPCURV(1,NU(1))=XL1
X=SPCURV(1,NU(4))
SPCURV(2,NU(1))=X
XX(6)=XX(6)+X-SPCURV(2,NU(4))
X=XX(6)/C2
SPCURV(3,NU(1))=X
C
XX(7)=XX(7)+X-SPCURV(3,NU(4))
X=XX(7)/C2
C
X=X+SPCURV(2,NU(3))+SPCURV(3,NU(2))
C
C REMOVE THE BIAS
C
XX=C1*BIAS
SPCV=X-XX
C
C SHIFT THE POINTERS
C
DO 150 I=1,4
NU(I)=NU(I)-1
IF(NU(I).EQ.0)NU(I)=256
150 CONTINUE
RETURN
END

```

```

SUBROUTINE JUMP(I,IBLK,IPRB,IACCEL)
C
C THIS SUBROUTINE REPLACES THE ACOUSTIC PROBE RANGE EXTENDER.
C IT DETECTS AND ELIMINATES JUMPS IN THE DATA DUE TO THE PHASE METER 360
C DEGREE RANGE. THE RANGE OF THE OUTPUT IS LIMITED ONLY BY THE
C COMPUTER'S INTEGER WORD LENGTH. THE OUTPUT IS DELAYED BY MAXSTP TIME
C STEPS.
C
      DIMENSION IDELAY(3,32)
      COMMON /IN/ IRAW(3,254)
C
C IMIN AND IMAX ARE THE MIN AND MAX THRESHOLDS (NEAR 0 AND 360 DEGREES),
C RESPECTIVELY. MAXSTP IS THE MAXIMUM NUMBER OF TIME STEPS SEARCHED
C FOR A JUMP. JUMPP IS THE INTEGER EQUIVALENT OF 360 DEGREES.
C
      DATA IMIN,IMAX,MAXSTP,JUMPP/60,1100,12,1169/,
      *IDELAY,JUMPS,NSTEP,LOLD,LO,IPTR/100*0,2/
C
C RAW DATA TAPE CHANNELS
C 1: BLOCK DISTANCE
C 2: NONCONTACT SENSOR
C 3: ACCELEROMETER
C
C INTRODUCE DELAY INTO DATA
C
      IPTR=IPTR-1
      IF(IPTR.EQ.0) IPTR=32
      LAG=IPTR+MAXSTP
      IF(LAG.GT.32) LAG=LAG-32
      IDELAY(1,IPTR)=IRAW(1,I)
      IDELAY(2,IPTR)=(IRAW(2,I)+JUMPS)
      IDELAY(3,IPTR)=IRAW(3,I)
      IBLK=IDELAY(1,LAG)
      IPRB=IDELAY(2,LAG)
      IACCEL=IDELAY(3,LAG)
C
C DETERMINE WHICH REGION WE ARE IN NOW
C
      LNEW=0
      IF(IRAW(2,I).GT.IMAX) LNEW=1
      IF(IRAW(2,I).LT.IMIN) LNEW=-1
C
C TEST FOR COMPLETION OF JUMP
C
      IF(LNEW*LO.LT.0.OR.LNEW*LOLD.LT.0) GO TO 100
      IF(LNEW.NE.0.OR.LOLD.EQ.0) GO TO 10
C
C START OF JUMP
C
      NSTEP=1
      LO=LOLD
      GO TO 20
      10 IF(LO.EQ.0) GO TO 20
C
C MIDDLE OF JUMP
C
      NSTEP=NSTEP+1
      IF(NSTEP.LT.MAXSTP) GO TO 20
C
C REINITIALIZE FOR A NEW JUMP
C
      15 NSTEP=0
      LO=0
C
C UPDATE AND RETURN
C
      20 LOLD=LNEW
      RETURN

```

```

C
C CALCULATIONS TO CORRECT FOR A JUMP
C
100 NSTEP=NSTEP+1
    JUMPS=JUMPS-JUMPP*LNEW
    IPN=IPTR+NSTEP
    IF(IPN.GT.32) IPN=IPN-32
    DO 110 J=1,NSTEP
        J1=IPN-J
        IF(J1.LT.1) J1=J1+32
C
C REPLACE ACOUSTIC PROBE DATA OVER JUMP INTERVAL WITH A STRAIGHT LINE
C
110 IDELAY(2,J1)=((NSTEP-J)*IDELAY(2,IPN)
    +J*(IDELAY(2,IPTR)-JUMPP*LNEW))/NSTEP
    GO TO 15.
    END

```

APPENDIX C
COMPUTER PROGRAM COMMON BLOCKS

COMMON/IN/	(Main and JUMP)
IRAW (3,256)	Digitized raw input data
COMMON/OUT/	(Main and OUTPUT)
IPROC (7,256)	Processed output data
COMMON/WORK/	(Main and OUTPUT)
IDOUT (7)	Seven output variables for each distance-based scan
COMMON/PAR/	(Main, SFD and BLKDIS)
FREQ	Digitization frequency (time-based)
RHO1	Coefficient used in SFD processing that depends on MODE
RHO2	Coefficient used in SFD processing that depends on MODE
OMA2	ω_a^2 , used in SFD processing
OMT2	$\omega_a T/2$, used in SFD processing
SCALE	Scale factor ratio (input)
COMMON/HW/	(Main and SPACEC)
NU (4)	Space curve pointers
C1	Space curve debiasing coefficient
C2	Space curve filter length, N

